# Characterizing Glucocorticoid-Induced Effects on Nuclear positioning, Microtubule Organization, and Microtubule Dynamics in Muscle Stem Cell and Myogenic Differentiation

by

**Leanne Dawe**

A thesis submitted to the University of Ottawa in partial fulfilment
of the requirements for the degree of
Master of Science: Medicine
In
Cellular and Molecular Medicine

Faculty of Medicine

University of Ottawa
Ottawa, ON, Canada

**ABSTRACT**

Duchenne muscular dystrophy (DMD) is the most common type of muscular dystrophy caused by the loss of functional dystrophin. DMD is characterized by scoliosis, muscle wasting, loss of ambulation and a reduced life span. The first line of treatment for DMD is glucocorticoids (GCs). GCs are prescribed primarily for their anti-inflammatory and immunosuppressive effects; however, GC treatment is known to cause significant muscle atrophy. In DMD, GC treatment has been shown to improve muscle strength for the first 6 months and stabilization of the disease for up to 3 years. However, long term treatment reduces muscle function and accelerates disease progression. It is paradoxical that we use a medication that causes muscle wasting to treat a muscle wasting disease. The regeneration and function of muscle is dependent on the proper regulation and functioning of muscle satellite cells (MuSCs) to restore and repair muscle tissue. The impact GCs have on MuSCs from activation to proliferation and differentiation into muscle fibers is not well understood. GCs have many mechanisms of action by acting as a ligand to the glucocorticoid receptor (GR) to cause downstream effects by direct DNA binding or indirectly by regulating proteins. To study the role of GCs, we examined the effects of GC treatment on myoblast morphology, the cytoskeletal network, post-translational modifications (PTMs) of tubulin subunits, and the organization of microtubule organizing centers (MTOCs) in proliferating and differentiating myoblasts. This study shows that the GR is an essential regulator of myotube morphology and proper myonuclei placement. Furthermore, dexamethasone (DEX) treatment causes branching of the MT network, as well as an increase in the expression of the stabilizing MT markers, acetylated and detyrosinated tubulin during early differentiation. DEX treatment was also found to misposition the Golgi complex, a primary MTOC for the cytoskeletal network, from the periphery of the nucleus to the center of the nucleus during early differentiation. Finally, we found very few differentially expressed genes between WT and $GR^{MuSC-/-}$ myoblasts between early and

late differentiation, indicating that these morphological defects we see are not due to GCs regulating gene expression. Thus, GCs act through the GR to modify the MT network during early differentiation, causing morphological changes in myoblasts that persist throughout differentiation.

**TABLE OF CONTENTS**

## LIST OF ABBREVIATIONS

| | |
|---|---|
| BSA | Bovine serum albumin |
| DBD | DNA binding domain |
| DEX | Dexamethasone |
| DGC | Dystrophin glycoprotein complex |
| DMD | Duchenne muscular dystrophy |
| DMEM | Dulbecco's modified eagle medium |
| EB | End binding |
| ECM | Extracellular matrix |
| EDTA | Ethylenediaminetetraacetic acid |
| FBS | Fetal bovine serum |
| FGF | Fibroblast growth factor |
| FIJI | Fiji Is Just ImageJ |
| GC | Glucocorticoids |
| GDP | Guanosine diphosphate |
| GE | Golgi elements |
| GR | Glucocorticoid receptor |
| GREs | Glucocorticoid response elements |
| GTP | Guanosine triphosphate |
| HDAC6 | Histone deacetylase 6 |
| HGF | Hepatocyte growth factor |
| HS | Horse serum |
| LBD | Ligand binding domain |

| | |
|---|---|
| LINC | Linker of nucleoskeleton and cytoskeleton |
| MACS | Magnetic activated cell sorting |
| MAPs | Microtubule associated proteins |
| MR | Mineralocorticoid receptor |
| MRFs | Myogenic regulatory factors |
| MTJ | Myotendinous junction |
| MTOC | Microtubule organizing complex |
| MTs | Microtubules |
| MuSCs | Muscle stem cells |
| Myf5 | Myogenic factor 5 |
| MyHC | Myosin heavy chain |
| MyoD | Myoblast determination protein |
| MyoG | Myogenin |
| NE | Nuclear envelope |
| NMJ | Neuromuscular junction |
| NTD | N-terminal transactivation domain |
| PAX7 | Paired box 7 |
| PBS | Phosphate-buffered saline |
| PFA | paraformaldehyde |
| PTMs | Post translational modifications |
| WT | Wild type |

**LIST OF FIGURES**

**ACKNOWLEDGEMENTS**

I would like to thank my research supervisor Dr. Nadine Wiper-Bergeron for her continued support and guidance throughout the past 2.5 years. Her constant encouragement and insight have been invaluable to the success of this research and to my personal and professional growth. I would also like to thank my co-supervisor Dr. John Copeland for his vital input and advice throughout the course of this project. Furthermore, I would like to extend my gratitude to my thesis advisory committee members, Dr. Rashmi Kothary and Dr. Laura Trinkle-Mulcahy. Their feedback and suggestions were crucial to the success of this project and to my professional development and skills as a researcher. I would like to thank all my fellow lab members in the NWB lab, with specific thanks to Dr. Hamood, Alsudais, Dr. Rashida Rajgara, Jocelyn Nguyen, Aisha Saleh, Alex Brown, Natasha Strong, and Hope Avramidis. Their constant encouragement, support, and friendship helped to motivate me throughout these past few years. I will forever cherish the many memories we have made both in and out of the lab. I would like to thank my dad, Leonard and my stepmom, Renee for their never-ending love and encouragement with every task I undertake throughout my life. I am grateful for my brothers, Allan and Brian, who have been the best friends I could ever ask for and for always keeping me on my toes. I am incredibly thankful for my husband Zach's constant love and support throughout all the ups and downs of this journey. I would like to thank my cat Nova for always reminding me that naps, play time, and good food are just as important as hard work. I am also grateful to all my incredible friends, Erin, Aimeer, Siny, Mary, Lulu, and Lumi for putting up with my late-night rants and constantly encouraging and supporting me. Furthermore, I would like to thank the UOttawa staff, including animal care and veterinary services, autoclaving, technical support, the graduate office, and the CMM secretaries for their assistance and hard work. All research at UOttawa is dependent on their dedication and I can't thank them enough for all that they do. I would also like to acknowledge the valuable contribution

of the mice that were used in this study. Their sacrifice to the progression of research and knowledge is invaluable and I am deeply grateful for their contribution to advancing our understanding of disease. Finally, I would like to acknowledge that the land on which this research was conducted is the traditional and unceded territory of the Algonquin Anishinaabe Nation. I recognize and deeply respect the knowledge and resilience of the Indigenous peoples who have lived on this land we now call home for thousands of years.

## CONTRIBUTION OF COLLABORATORS

This research was supported by a grant from the Canadian Institutes of Health Research (CIHR) to Dr. Nadine Wiper-Bergeron (NWB). Leanne Dawe is supported by the Ontario Graduate Scholarship (OGS) from the University of Ottawa, ON. Analysis of microtubule dynamics and cytoskeletal staining using imaging facilities was performed with the assistance of Dr. John Copland. Previous and present lab members including Dr. Hamood Alsudais, Dr. Rashida Rajgara, Jocelyn Nguyen, Aisha Saleh, Alex Brown, Natasha Strong, Hope Avramidis, Ayesha Syed, and Mariam Almasaad for their support and assistance with sample collection, data processing and quantification. The Cell Biology and Image Acquisition Core (CBIA Core) and their staff members Dr. Chloë Van Oostende-Triplet and Liyuan Wang, funded by the University of Ottawa, Ottawa, Natural Sciences and engineering Research Council of Canada, and the Canada Foundation for Innovation for help with image acquisition, processing, and analysis. Genome Quebec (Montréal, QC) for library preparation and bulk RNA sequencing.

# 1. INTRODUCTION

## 1.1 Muscle stem cells and myogenic differentiation

Skeletal muscles are striated muscle tissues that form nearly 40% of the body mass. The regeneration of skeletal muscle in response to stress, injury, or wasting relies on stem cells called muscle satellite cells (MuSCs)[1-5]. MuSCs are located between the basal lamina and the myofiber plasma membrane[6]. These quiescent stem cells are characterized by their expression of Paired box 7 (PAX7)[7-10]. Myogenic differentiation is primarily carried out by the helix-loop-helix family of transcription factors called myogenic regulatory factors (MRFs)[11]. MRFs include MYF5, MYOD, MYOG, and MRF4 that are expressed at different time points throughout differentiation (Fig. 1B)[11]. When injury, exercise, or disease cause muscle damage, MuSCs are activated to proliferate and induce expression of MYOD and MYF5 before exiting the cell cycle and committing to differentiation and upregulating MyoG[12]. The combination of MyoD and MyoG then leads to the expression of MRF4, permitting the multinucleation of myofibers[11]. Once mature, the expression of MyoD and MyoG is downregulated, while MRF4 expression remains high[11]. Myogenic differentiation is also characterized by the fusion of differentiated myoblasts to each other to form new myofibers or with damaged fibers to regenerate the damaged muscle along with the expression of the structural and contractile proteins myosin heavy chain (MyHC) (Fig1. A)[13-15].

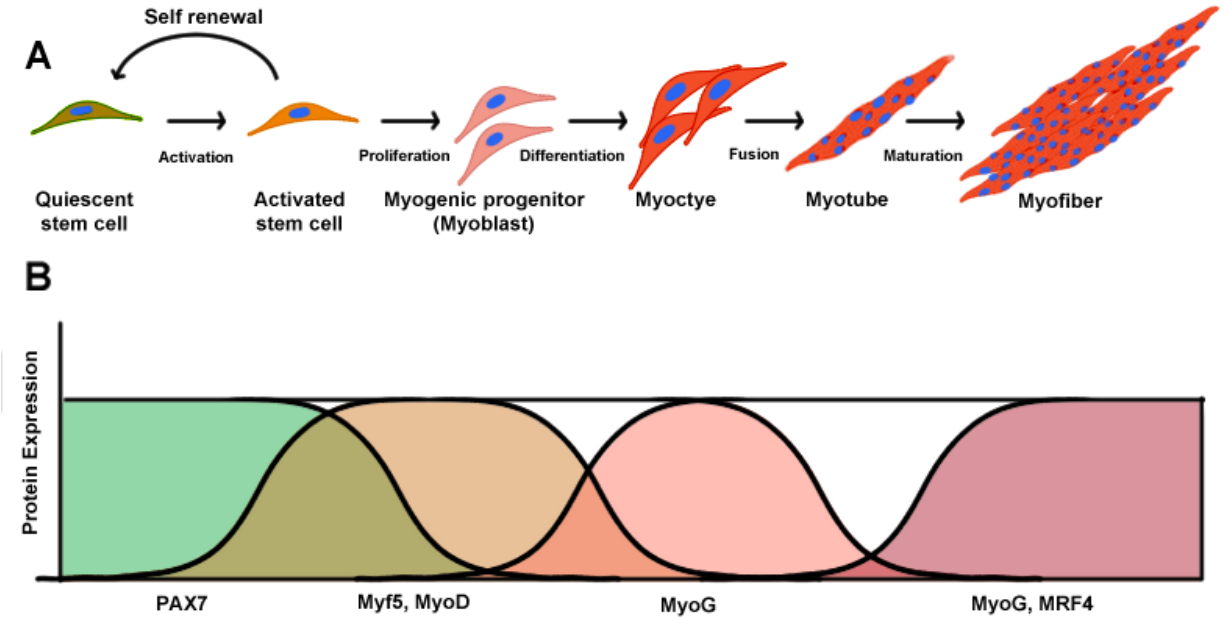


**Figure 1. Transcriptional regulation of adult skeletal myogenesis. (A)** A schematic representation of the molecular and cellular events involved in adult muscle stem cell activation and differentiation into skeletal muscle. When muscle fibers are damaged due to injury, exercise, or disease, MuSCs (PAX7+) exit quiescence and proliferate into myoblasts (Myf5+, MyoD+). After expansion, myoblasts differentiate and express MyoG, then fuse to form new fibers or fuse with existing muscle fibers to repair damaged tissue. A proportion of MuSCs undergo self-renewal to repopulate the MuSC niche. **(B)** Graphical depiction of protein expression of transcription factors. Created with BioRender.com

## 1.2 Cytoskeletal and nuclear changes during myogenic differentiation

As myoblasts differentiate, coordinated events of subcellular remodeling affect the nuclei, microtubules (MTs), centrosome, and the Golgi complex[16]. As myofibers fuse and mature post regeneration, successive nuclear movements and positioning events place myonuclei at the periphery of the cell under the plasma membrane (Fig. 2A)[17]. Successive positioning events are driven by the cytoskeletal network in connection with the nuclear envelope (NE)[17].

Microtubules are polarized dynamic polymers comprised of heterodimers of α-tubulin and β-tubulin that form a hollow tube filament structure[18]. MTs are an integral part of the cytoskeleton and are essential to maintaining the structure and function of cells[19]. This includes forming the

mitotic spindle, axonemes of cilia and flagella, intracellular trafficking, and the maintenance of cellular architecture to form cell shape, maintain polarity, and organelle positioning[19]. There are two major microtubule organizing centers (MTOCs) from which MTs originate – the centrosome and the Golgi complex[20]. The majority of MTs emanate from the centrosomal MTOC and its main role is to ensure the proper formation and positioning of the bipolar spindle during cell division[18]. However, for different cell types to perform specific functions, their MT network may reorganize to meet these demands and MTs become organized from other subcellular sites like the Golgi Complex[19]. Skeletal muscle cells retain vestigial MTOC activity at the centrosomes, while the main MTOC functions are carried out by non-centrosomal sites like the Golgi Complex. MTs are essential for Golgi integrity and the positioning and orientation of the MT network works in tandem with proper Golgi positioning to define a secretory axis[19].

As myoblasts fuse with myotubes, the Golgi complex is distributed to the NE, colocalized with endoplasmic reticulum exit sites and broken apart into Golgi elements (GE)[16]. These GE are positioned at vertices of the MT lattice network and serve as a MTOC to nucleate these structures[16]. MTs nucleated from Golgi elements grow along other MTs to form an orthogonal grid network by associating with dystrophin at the membrane[16,21]. It is unknown whether there is a functional difference between MTs nucleated from the nuclei or Golgi elements[16]. GE positioning is abnormal in the absence of dystrophin, but dystrophin is not necessary to anchor the GE[21]. Studies show that mispositioning of these GE and the random orientation of MTs cause disorder in the MT network in cells lacking dystrophin[21]. Therefore, dystrophin may play an indirect role in positioning GE.

MT dependent nuclear movements involve pushing and pulling from the MTOC bound to the NE[17]. After myocyte fusion, the first positioning event is termed “nuclear centration”, where

the nucleus from the fusing myocyte rapidly moves towards the center of the nascent myotube[17,22]. Centration of the nuclei is driven by MTs and regulated by Cdc42 and polarity proteins Par6 and Par3 (Fig. 2B)[17]. Subsequently, "alignment" occurs, where the myonuclei align along the long axis of the myotube. The third event is "elongation", where myonuclei migrate longitudinally from the center of the fiber to the periphery to become evenly spaced as the myotube matures into a myofiber[23-25]. Next, "peripheral movement" occurs, where the myonuclei migrate from the center of the cell to the periphery and become anchored below the plasma membrane of the myofiber[24,25]. During the "alignment" and "anchoring" stage, the interaction between Kif5b/Kinesin-1 and Map-7 maintains an anti-parallel MT network (Fig. 2C)[17]. The force on this network exerted from Kinesin-1 towards the (+) end allows nuclei to align and evenly spread[17]. Nesprins and SUN proteins are involved in peripheral movement and anchoring of myonuclei to the periphery of the fiber[17]. Some myonuclei also cluster under neuromuscular junctions (NMJ) and the myotendinous junctions (MTJ) to specifically express mRNAs encoding proteins that are involved in synapse communication[17]. These junctions are the chemical synapses between motor neurons and muscle cells and are essential for proper muscle contraction and movement[26]. Improper functioning of these junctions leads to neuromuscular disease[26].

Nuclear migration is highly dependent on MT-associated motor proteins called dynein and kinesins[17]. The centrosomes disassemble and pericentriolar proteins (pericentrin and Cep135) are brought to the nuclear envelope (NE) by Nesprin1α, which switches the MTOC to the NE[27]. Nesprin1α is a component of the linker of nucleoskeleton and cytoskeleton (LINC) complex[27]. LINC complex integrity is essential for proper myonuclei positioning during myoblast fusion and differentiation to transport centrosomal proteins to the NE[27]. Nesprin-1 is also critical in the anchoring of myonuclei by allowing a bridge between myonuclei and actin in the cytoskeleton[27].

After fusion of a myoblast to a myotube, the nuclear movement involves MTs emanating from myotube nuclei to bind the NE of new nuclei through dynein anchored by the polarity complex protein, Par6[17]. The accumulation of Par6 and dynein/dynactin complex components at the NE of myoblasts is dependent on Par6β but not MTs, suggesting that Par6β is an anchoring partner for dynein/dynactin[17].

Centration results from nuclei pulling nucleated MTs from the NE of other nuclei[17]. Cdc42 and Par3 are also regulators of this process[17]. During myogenesis, centrosomal proteins accumulate at the NE in myofibers to form nucleating centers and allow direct nucleation and formation of MTs[28,29].

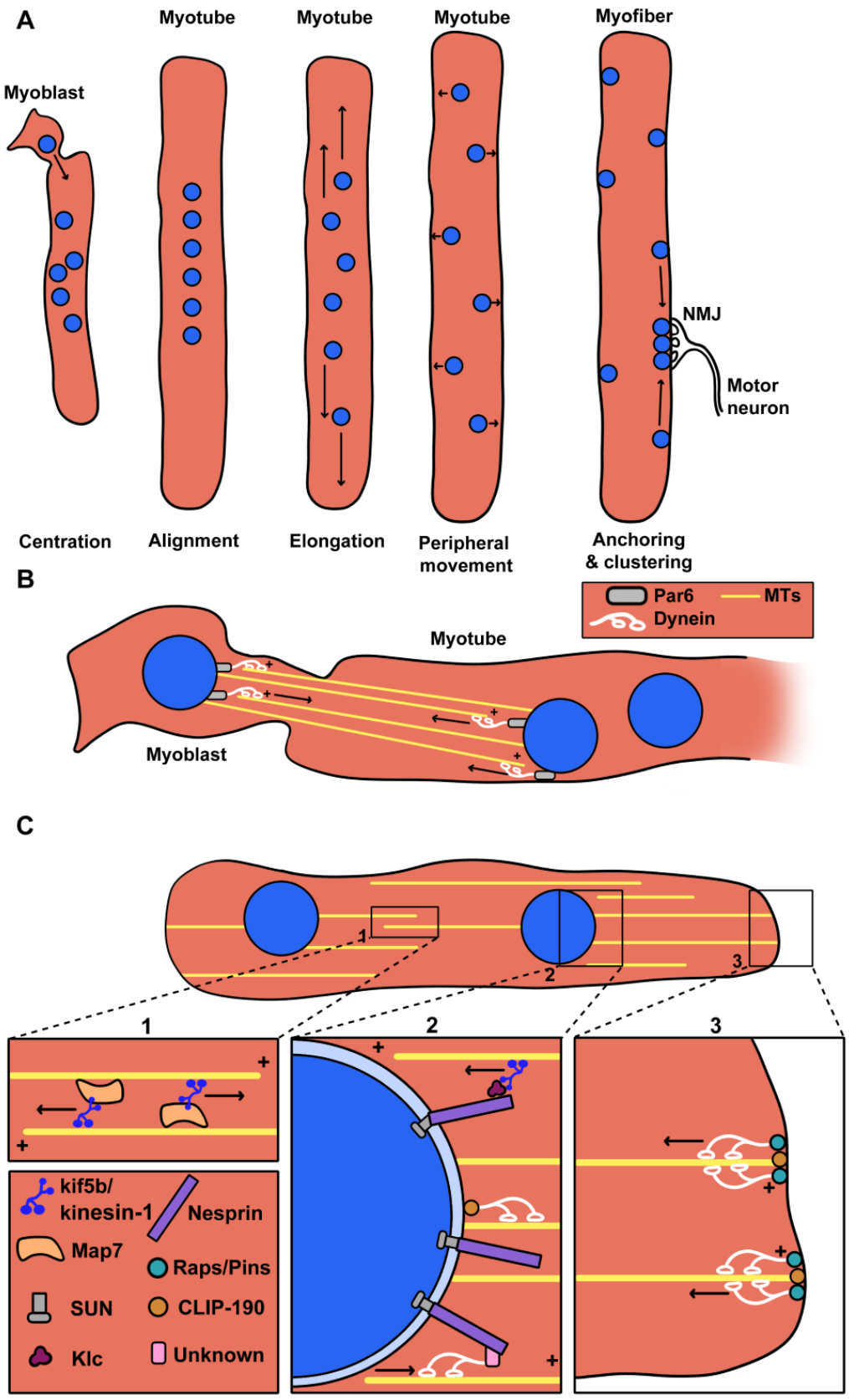
A
Myoblast
Myotube
Myotube
Myotube
Myofiber
NMJ
Motor neuron
Centration
Alignment
Elongation
Peripheral movement
Anchoring & clustering
B
Par6
MTs
Dynein
Myotube
Myoblast
C
1
2
3
kif5b/ kinesin-1
Nesprin
Map7
Raps/Pins
SUN
CLIP-190
Klc
Unknown

**Figure 2. Nuclear movements during myoblast fusion. (A)** A schematic representation of myoblast fusion where myoblasts merge to form multinucleated myotubes. Centration occurs when the myoblasts fuses with a myotube and the nucleus from the myoblast migrates to the center of the myotube. Alignment is the arrangement of these nuclei along the central longitudinal axis. Elongation is the longitudinal movement of the myonuclei along the cell as the myotube elongates into a fiber. Peripheral movement is the migration of these nuclei from the center of the cell to the periphery below the plasma membrane. Anchoring occurs when these nuclei become secured under the plasma membrane with some clustered beneath the neuromuscular junction. **(B)** A schematic representation of Centration, where the nucleus of a fusing myoblast is pulled to the center of the myotube by the attachment of Par6-dynein to the MTs emanating from the myotube nuclei. **(C)** A representation of alignment, elongation, and peripheral movement. Alignment occurs by the pushing and pulling motion of myonuclei with the assistance of kif5b/kinesin-1 and Map7 that "walk" along the antiparallel MT network to position myonuclei at the center of the myotube. Elongation along the long axis of the myotube is achieved by the Sun-Nesprin proteins attaching to the MT network by dynein or KIc-kif5b/kinesin-1 to pull the myonuclei to the far edge of the myotube. Adapted from: Moving and positioning the nucleus in skeletal muscle - one step at a time. By Cadot B, Gache V, Gomes ER. Nucleus. 2015;6(5):373-81. doi: 10.1080/19491034.2015.1090073. PMID: 26338260; PMCID: PMC4915500. Created with BioRender.com

### 1.3 Microtubules and Post-translational modifications during myogenic differentiation

MTs are dynamic polymers of α, and β tubulin heterodimer subunits assembled into linear protofilaments[20]. These protofilaments form a polarized spiral tube where the (-) end of the MT has α-tubulin subunits exposed, and the (+) end has β- tubulin subunits exposed[18]. While both ends of the MT switch between phases of growth and shrinkage, a behavior termed "dynamic instability", elongation is significantly more rapid at the (+) end (Fig. 3)[18,30]. The varying instability of MTs allows for both stable and dynamic MT networks[20]. MTs grow by the addition of guanosine triphosphate (GTP) conjugated tubulin to the heterodimers at the (+) end of the MT (Fig. 3)[20]. This GTP stabilizing cap is formed on the (+) end of the MT to promote MT elongation[18]. The GTP-enriched tubulin cap recruits end binding (EB) proteins and other MT-associated proteins (MAPs), such as MT polymerase, depolymerases, and kinesins that determine the fate of the MT[18]. Once this cap is lost by GTP hydrolysis, the MT undergoes rapid shrinking ("catastrophe") and can be "rescued" from this state and switched back to growth[18].

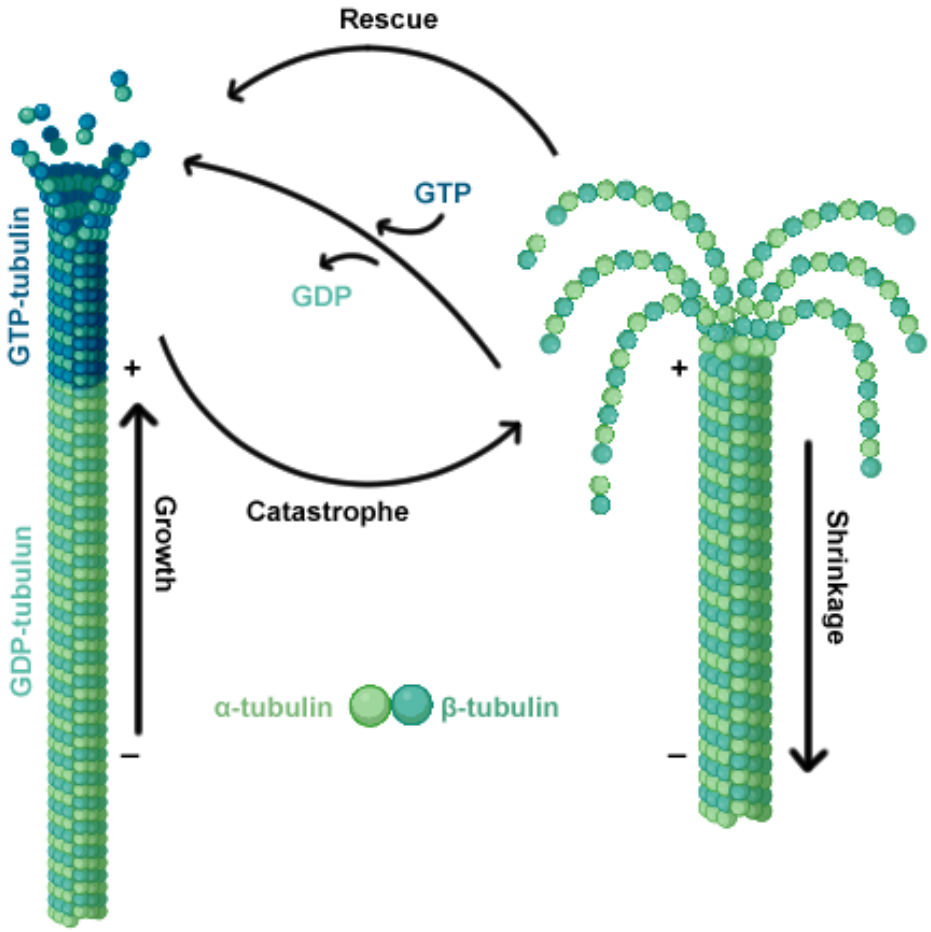


**Figure 3. Microtubule formation and structure.** MTs are dynamic polymers of α, and β tubulin heterodimer subunits assembled into linear protofilaments. The αβ-heterodimers are added to the (+) end of the MT (polymerization) and removed from the (-) end (depolymerization) The constant state of MT growth and shrinkage is known as dynamic instability. A GTP enriched cap at the (+) end of the MT stabilizes the growth phase, and when this cap is lost due to GTP hydrolysis, the MT undergoes catastrophe and shrinkage. Created with BioRender.com

Some MTs persist for hours while others are very unstable and disassemble within minutes[20]. Maintaining these dynamics is essential for cell function, as MTs contribute to cell organization by providing a scaffold for intracellular transport and exerting forces on subcellular structures[19]. The two major factors contributing to the dynamic instability of MTs are the post translational modifications (PTMs) of tubulin, and interactions with MAPs[20]. PTMs are one of the main factors contributing to MT dynamics on tubulin subunits, often by regulating the interactions

of MTs with MAPs[20]. The main PTMs that have been studied to date are tyrosination, detyrosination, acetylation, and polyglutamylation[30].

Tyrosine is the most frequent amino acid residue on the α-tubulin C-terminal end that can be removed and incorporated into MTs by a carboxypeptidase (detyrosination) to form Glu-tubulin[20]. Detyrosination stabilizes MTs by preventing depolymerization by inhibiting kinesin-13 and by reducing MT growth, allowing detyrosinated MTs to persist for hours[19]. Detyrosinated MTs also regulate muscle contractility by providing resistance to shortening of the sarcomere during muscle contractions[19]. Inhibiting detyrosination increases the shortening and contractile velocity of muscle cells, however, an increased level of detyrosination leads to cell rigidity and may increase muscle damage due to breakage during muscle contractions[19]. The levels of detyrosination in proliferating myoblasts are low, but once induced to differentiate, there is rapid accumulation of detyrosinated MTs that precedes the accumulation of muscle myosin[31]. Myotubes at late stages of differentiation continue to maintain an elevated level of detyrosination[31]. The proper balance of detyrosinated tubulin maintains the muscle cell cytoskeletal network so cells are not too rigid and prone to breakage upon contractions, and not so flexible that they are too weak to resist contraction forces[19].

Acetylation is a highly conserved tubulin modification that occurs most often on the lysine 40 residue of α-tubulin subunits[20]. The primary acetyltransferase for K40 is αTAT1, while the deacetylases are Sirt2 and Histone deacetylase 6 (HDAC6)[20]. αTAT1 enters the lumen at the MT ends, initiating acetylation and slowly diffusing inside the MT, limiting the rate of acetylation by the slow catalytic activity of αTAT1[20]. HDAC6 is a MAP that also regulates MT dynamics by deacetylating α-tubulin and can cause hypoacetylation when overexpressed and hyperacetylation when inhibited[32]. HDAC6 binds to β-tubulin to deacetylate lysine 40 on the neighbouring α-tubulin

subunit and becomes uncoupled from β-tubulin upon completion[32]. Acetylation is initiated at the ends of the MTs, and the acetylated segment enlarges as the MT elongates[20]. Acetylation enhances MT flexibility by weakening their lateral interactions with neighbouring MTs to protect them from breakage and mechanical ageing due to repetitive contractions and bending[19]. By weakening these lateral interactions, acetylation increases plasticity of the MT network, limiting the spread of lattice damage under repeated mechanical stress, protecting MTs from mechanical fatigue[20]. Thus, deacetylated MTs break more frequently than acetylated MTs[20]. Acetylated MTs were also shown to be more resistant to cold shock and depolymerizing agents like nocodazole[20]. Acetylation also increases upon differentiation, but only after the fusion of myoblasts[31].

Polyglutamylation regulates the interactions of MTs with other MAPs as well as modulates the severing of MTs by spastin and katanin[19]. Polyglutamylation is the addition of 1-6 glutamyl units to both α-and β-tubulin subunits[19]. These PTMs help to establish an oriented lattice of stable MTs that is essential for subcellular remodeling during myognesis[31].

### 1.4 Duchenne Muscular Dystrophy

Duchenne muscular dystrophy (DMD) is the most common type of muscular dystrophy and affects 1 in every 3500 males[33]. DMD is caused by an X-linked nonsense mutation in the gene encoding dystrophin, a structural protein found on the cytoplasmic surface of skeletal muscle cell membranes[34]. Loss of functional dystrophin causes instability of the plasma cell membrane (sarcolemma) and myofiber loss[35]. Dystrophin binds with other proteins to form the dystrophin glycoprotein complex (DGC)[35]. The DGC is comprised of 3 protein groups based on their cellular position: extracellular (α-dystroglycan); transmembrane (β-dystroglycan, sarcoglycans, sarcospan); cytoplasmic (dystrophin, dystrobrevin, syntrophins, neuronal nitric oxide synthase)[35]. The DGC connects the intracellular cytoskeleton to the extracellular matrix (ECM) to act as a

membrane stabilizer during muscle contraction, preventing contraction-induced damage[35]. In the cytoplasm, dystrophin maintains the sarcolemma membrane localization by interacting with β-dystroglycan and binding to the intracellular actin network, linking the cytoskeleton to the DGC[35]. The DGC also mediates cellular signaling, such as mechanical force transduction and cell adhesion[35].

DMD is characterized by scoliosis, muscle wasting, loss of ambulation, and a reduced life span[36-38]. The absence of dystrophin results in decreased muscle fiber strength, myofiber necrosis, and abnormal stem cell function[36-38]. Petrof et al. found that dystrophin-deficient muscle fibers have an increased risk of contraction-induced sarcolemma rupture that is correlated with the magnitude of mechanical stress[34]. This indicates that one of dystrophins primary functions is to provide mechanical support to the sarcolemma during muscle contractions, and when dystrophin is lost, this causes the lack of muscle fiber strength[34]. This was further supported with data from Moens et al., who found through histological analysis that muscle lacking dystrophin has a 40-60% decrease in force production that is associated with membrane damage and muscle degradation[37]. Furthermore, Dumont et al. found that dystrophin is essential for regulating the polarity and asymmetric division of MuSCs, exacerbating the already impaired stem cell function in DMD[38].

DMD patients treated with glucocorticoids (GCs) have improved muscle strength, ambulation, and cardiac function for the first 6 months of treatment and disease stabilization for up to 3 years[39]. However, given that GCs are involved in multiple mechanisms, it is unclear which molecular pathways mediate the positive and negative effects[39]. Despite the positive effects seen with short-term, low-dose treatment of GCs, long-term treatments reduce muscle function and accelerate disease progression[40,41]. Alternative anti-inflammatory therapies that decrease

intramuscular infiltration by immune effector cells are shown to be less effective than GCs, inferring that GCs have benefits outside of the immune system that contribute to clinical efficacy[42]. In 2015, the McNally group showed that weekly doses of GCs improve DMD symptoms by direct transactivation of a downstream transcription factor KLF15[43]. Also, GCs were shown to increase expression of annexin A1 and A6, which mediate myofiber repair by promoting membrane resealing[43]. However, when they investigated the impact of various doses of GCs, they found that daily treatment resulted in decreased force generation and increased atrogene expression, which is known to induce muscle atrophy[44]. Meanwhile, weekly treatments exhibited an increased force generation and no increase in atrogene expression[44]. GC treatment also increases the expression of utrophin, which stabilizes the muscle membrane in the absence of dystrophin[45,46]

### 1.5 Glucocorticoids

GCs are naturally occurring steroid hormones produced by the adrenal cortex and released in response to stress and various biological cues. The primary function of glucocorticoids is the regulation of glucose metabolism, but they also play a role in regulating inflammation, cognition, development, skeletal growth, the cardiovascular system, and reproduction[47]. GCs are widely used therapeutically due to their immunosuppressive and anti-inflammatory actions[48]. GCs suppress the immune system by sequestering CD4+ T-lymphocytes throughout the reticuloendothelial system and inhibiting the transcription of inflammatory cytokines, like IL-2, IL-3, IL-4, IL-5, IL-6, TNFα, GM-CSF, CCL1, CCL5, CCL11, and CXCL8 [49]. Thus, GCs treat various diseases, such as autoimmune disease, arthritis, muscular dystrophies, and cancers by suppressing the immune system and reducing inflammation[49]. However, steroid use has been shown to cause side effects including muscle atrophy and osteoporosis, that both increase muscle weakness and frailty[50].

There are a variety of both natural and synthetic GCs. Natural GCs like cortisol are derived from cholesterol and secreted by the adrenal cortex to maintain glucose homeostasis[51]. Synthetic GCs such as Dexamethasone (DEX), Deflazacort, and Prednisone were produced for pharmacological purposes due to their anti-inflammatory properties and are a useful tool in studying the unknown effects of GCs on various cell types[51]. GCs are the standard treatment for patients with DMD[52]. Paradoxically, the primary treatment for a muscle wasting disease is a drug that itself causes muscle atrophy.

### 1.6 The glucocorticoid receptor

The functions of GCs are carried out by the glucocorticoid receptor (GR), an intracellular modular protein that is a member of the nuclear hormone receptor family, encoded by the *Nr3c1* gene[53]. This ligand-activated transcription factor is comprised of 3 major functional domains: a N-terminal transactivation domain (NTD), a central DNA binding domain (DBD), and a C-terminal ligand-binding domain (LBD)[53]. The DBD is the most conserved domain and binds to DNA target sequences called glucocorticoid response elements (GREs)[53]. When GCs are absent, GR is found in the cytoplasm as a component of a multi-protein complex including heat shock proteins (hsp90 and hsp70), immunophilin proteins (FKBP51 and FKBP52), and various other proteins[54,55]. Once bound to GCs, the GR undergoes a conformational change and dissociates from the heat shock proteins, exposing the nuclear localization signal[56]. This allows for the translocation of the GR receptor into the nucleus through the nuclear pores[57]. Once inside the nucleus, GR binds directly to GREs in the promotor and enhancer regions of the target gene to either upregulate or downregulate the transcription rate of GC-responsive genes[58-60]. After modulating transcription of GC-responsive genes, GR dissociates from the ligand and gradually returns to the cytoplasm to reform heterocomplexes[61]. GR function has also been shown to modulate transcription

independently of direct binding to DNA[61]. GR can stimulate or inhibit transcription rates of target genes by protein-protein interactions with specific transcription factors, allowing transcription from promoters that do not contain GREs[61]. This is observed particularly in inflammation and immune system suppression where GR interacts with the transcription factors NF-kB, AP-1, and STATs[62-64].

GR can also recruit coactivator and corepressor proteins such as histone deacetylase (HDACs)[65] and can regulate microtubule dynamics by binding directly to the MTs or indirectly by inhibiting HDAC6[66,67]. Kershaw et al. found that the GR activated by the presence of GCs inhibits HDAC6 function and increases the stability of the MT network by increasing the acetylation levels of tubulin subunits[66]. They identified a cytoplasmic interaction between GR and HDAC6 with a 5-fold increase in interaction strength upon DEX treatment when compared to control[66]. They also identified a rapid increase in MT polymerization with the onset of GC treatment that was brought to baseline levels with the overexpression of HDAC6, indicating that GCs act through the GR to stabilize the MT network by inhibiting HDAC6 and increasing acetylation of MT subunits[66]. However, hyperacetylation of transcription factors and nuclear cofactors by histone acetyltransferases (HATs) may render these proteins susceptible to degradation to influence muscle mass and wasting[65]. There is an imbalance between HAT and HDAC levels during muscle wasting, which directly influences acetylation levels and provides yet another potential mode of action where GCs regulate muscle mass independent of direct DNA binding[65].

Furthermore, the glucocorticoid receptor (GR), MYOD1, and NRF1 interact with each other and play an essential role in myofiber gene regulation to control myofiber size[68]. MYOD1 is recruited to muscle enhancers in domains centered on GR binding sites that are GR dependent[68]. The presence of MYOD1 is required for GR binding that contributes to GR-regulated anti-anabolic

transcription, limiting muscle fiber size[68]. GR also interacts with NRF1 in the nucleus, regulating the transcription of GR target genes in myofibers[68]. Thus, illustrating another way that GCs can improve muscle fiber function and stem cell endurance by acting through the GR to regulate transcription. Given the many pathways' GCs play a role in and the variability in short-term and long-term effects, more research and understanding of GC treatment in DMD is necessary.

The GR is also an essential regulator during cell division[69]. In quiescent cells, GR is nearly exclusively located in the cytoplasm and only translocates into the nucleus upon GCs binding, while live cell imaging revealed significant import of GR into the nucleus during interphase without ligand binding[70]. However, with the onset of mitosis there is an enrichment of GR to the mitotic spindle and GR knockdown causes an accumulation of mitotic spindle defects, such as delayed anaphase, ternary chromosome segregation and apoptosis[69] Tissues deficient in GR enriched mitotic spindles show an increase in aneuploidy and DNA damage, and this loss of GR expression has been observed in various common cancers (liver, lung, prostate, colon, and breast)[70]. This reveals a non-transcriptional and ligand-independent mechanism of action of the GR that causes accurate chromosome segregation during mitosis.

The proper functioning of skeletal muscle is highly reliant on the morphology of mature myotubes. Abnormalities such as centrally located myonuclei and a disorganized MT network are associated with muscular diseases like DMD. The GR regulates various functions in muscle development by interacting directly with DNA to alter transcription or indirectly by interacting with regulatory proteins to control gene expression and post-translational modifications to modify cell morphology and function. Thus, the use of GCs in treating DMD is of interest. My research will explore the impact GCs have on the nuclear positioning, MTOC positioning, and MT

dynamics of skeletal muscle stem cells to uncover potential cellular mechanisms that may cause muscle wasting and fragility.

To examine the effects of glucocorticoid treatment on myoblast differentiation and fusion, our lab differentiated primary myoblasts in the continuous presence of the synthetic glucocorticoid (DEX) at different concentrations. Myosin heavy chain (MyHC) immunostaining revealed an overall increase in both myogenic differentiation and fusion in increasing concentrations of DEX and while DEX enhanced myogenic cell fusion, it also caused gross abnormalities in myotube morphology, characterized by large myotubes with multiple elongated projections[95]. By contrast, primary myoblasts lacking GR were able to differentiate and fuse with the same efficiency as WT controls, but the fused cells were more rounded with clustered myonuclei.

### 1.7 Rationale & Hypothesis

Nuclear positioning is a MT-dependent process. The abnormal, branched myotube morphology observed in cultures differentiated in the presence of GCs suggests that GCs are an essential regulator of the myotube cytoskeleton. We hypothesize that GCs act through the GR to regulate the cytoskeleton, including nuclear positioning, MTOC organization, and MT network dynamics during myoblast growth and differentiation. My findings provide insight into the specific structural components that are altered by GCs and will provide essential information about which pathways induce muscle wasting from GC use and which are responsible for the beneficial effects.

## 2. MATERIALS AND METHODS

### 2.1 Mice and Animal Care

All animal work was performed within the guidelines set out by the Canadian Council on Animal care and approved by the University of Ottawa Animal Care Committee. The conditional knockout of GR (*Nr3c1*) in muscle stem cells ($GR^{MUSC-/-}$) was generated by breeding the $Pax7^{CreERT2}$ mouse [Jackson Labs, strain# 017763, $Pax7^{tm1(Cre/ERT2)}$ Gaka] with a floxed *Nr3c1* mouse ($GR^{fl}$) [Jackson Labs, strain# 021021, B6.Cg-$Nr3c1^{tm1.1Jda}$/J]. The Cre recombinase is expressed by the $Pax7^{CreER}$ allele and is under the control of the Pax7 promotor, which allows for the normal protein expression of PAX7. Tamoxifen treatment of these mice induces the nuclear translocation and interaction of Cre with *loxP* sides to excise exon 3 of the *Nr3c1* gene, knocking out GR expression in $Pax7^{+}$ cells (muscle stem cells). Both ($Nr3c1^{fl/fl}$; $Pax7^{CreERT2/+}$; $GR^{MUSC\ -/-}$) and control mice ($Nr3c1^{fl/fl}$: $Pax7^{+/+}$; WT) were generated at Mendelian ratios. All animals were housed in a controlled facility at the University of Ottawa. Housing conditions were kept at a constant temperature of 22°C and 30% relative humidity on a 12-hour light/dark cycle. Food and water were provided *ad libitum*.

### 2.2 Cell Culture

Primary myoblasts were isolated from 6–8-week-old male and female WT ($Nr3c1^{fl/fl}$: $Pax7^{+/+)}$ and $GR^{MUSC-/-}$ ($Nr3c1^{fl/fl}$; $Pax7^{CreERT2/+}$) mice that were treated with tamoxifen (dissolved in corn oil) at a concentration of 2.5mg/kg of body weight intraperitoneally (i.p) for 5 consecutive days. These mice were left to rest for one week without treatment to avoid any recombinant escapers before collecting cells using Magnetic Activated Cell Sorting (MACS)[71]. The lower hindlimb muscles were collected and digested with 0.2% collagenase type II (Worthington Biochemical Corporation, Lakewood, NJ) in Dulbecco's Modified Eagle Medium (DMEM,

Thermo fisher Scientific, Massachusetts, USA) for 1.5 hours. The muscle slurry was filtered through a 70μm cell strainer to remove undigested muscle and other contaminants. The cell solution was washed with MACS buffer, consisting of 0.5% bovine serum albumin (BSA) and 2mM ethylenediaminetetraacetic acid (EDTA; Bioshop Canada Inc., Ontario, Canada) in phosphate-buffered saline (PBS). Cells were magnetically tagged for 15 mins by incubating on ice in the dark using the mouse satellite cell isolation kit (Miltenyi Biotec, Gladbach, Germany). This kit contains magnetic beads conjugated to a cocktail of monoclonal antibodies against non-target cells (CD45, CD31, CD11b, and $Sca1^-$). Cells were passed through a MACS separation (LS) column to magnetically separate non-labelled muscle stem cells from the labelled non-target cells (negative selection). The flow through was collected and the labelled non-target cells remained in the MACS column and were discarded. To further sort the eluted cells, they were plated on a 10cm dish for one hour in growth medium (GM) containing DMEM, 20% Fetal Bovine Serum (FBS), 10% Horse Serum (HS), 1% Penicillin/Streptomycin (Wisent, Quebec, Canada). This removes any non-target cells, such as endothelial cells, blood cells, and fibroblasts, that may have passed through the column by allowing them to adhere to the plate, while primary myoblasts remain in the suspension. Cells like fibroblasts have integrins on their cell surface, allowing for their quick attachment to the culture plate, while primary myoblasts remain in suspension[72]. The suspension containing isolated satellite cells were then plated on dishes coated with Matrigel (Corning Discovery Labware, Bedford, MA) and supplemented daily with 10ng/mL basic fibroblast growth factor (FGF) and 2ng/mL hepatocyte growth factor (HGF) (Peprotech, Rocky Hill, NJ). Cell cultures were treated with Dexamethasone (DEX; Sigma-Aldrich) daily at a concentration of 1uM in 100% ethanol; which 100% ethanol was used as the vehicle control. Cells were grown and maintained in a humidified water-jacketed incubator at 37°C and 5% $CO_2$.

C2C12 (immortalized myoblast cell line, ATCC, Manassas, VA) cell stock solutions previously stored in liquid nitrogen were thawed in a 37°C water bath and plated on a 10cm dish in growth medium (GM) containing DMEM, 10% Fetal Bovine Serum (FBS) and, 1% Penicillin/Streptomycin (Wisent, Quebec, Canada). Cells were grown and maintained in a humidified water-jacketed incubator at 37°C and 5% $CO_2$.

### 2.3 Immunostaining and Antibodies

Primary myoblasts and C2C12 cells were fixed in 4% paraformaldehyde (PFA) for 15 minutes and permeabilized with 0.5% Triton X-100 in PBS and 10% goat serum. Cells were incubated with primary antibodies such as myosin heavy chain (pan MF20 antibody), GM-130 (anti-mouse, cat: 610822, BD Biosciences, New Jersey, USA), Pericentrin (anti-mouse, cat: 611814, BD Biosciences, New Jersey, USA), detyrosinated tubulin (anti-rabbit, AB3201, Milipore Sigma, France), acetylated tubulin (anti-mouse, T7451, Sigma-Aldrich, Missouri, USA) overnight at 4°C. The cells were then washed 3x in 0.1% Triton X-100 in PBS and incubated with fluorescent-conjugated secondary antibodies such as Cy3 anti-mouse, and Alexa Flour 488 anti-rabbit (AB2315777, AB2338052, Jackson ImmunoResearch, West Grove, PA) for one hour in the dark at room temperature. The cells were then washed 3x in 0.1% Triton X-100 in PBS and counterstained with 4',6-diamidino-2-phenylindole (DAPI; Fisher Scientific, Eugene, OR) (0.5 μg/mL) at room temperature for 5 minutes, then mounted in Dako fluorescence mounting medium (Agilent Technologies, Glostrup, Denmark) on glass slides (Fisherbrand, Pittsburgh, USA). All images were taken on the Zeiss AxioObserver 7 (CBIA Core, UOttawa) and analysis completed using Fiji.

## 2.4 Western Blot

To collect cells, media was aspirated, and cells were washed and scraped in PBS. The cells were spun down at 3,000g for 3 mins. The supernatant was removed, and the cell pellet was lysed in IPH lysis buffer (50 mM Tris–HCl pH 7.5, 150 mM NaCl, 5 mM EDTA, 0.5% NP-40) supplemented with 100 mM PMSF and 100 mM DTT (Dithiothreitol, Sigma Aldric). Lysates were agitated for 30 minutes at 4°C on a shaker and centrifuged at 17,000g for 10 minutes. The whole cell extract (supernatant) was collected, and the pellet discarded. Whole cell extract was separated on 4-15% mini-PROTEAN TGX Precast Protein Gels (Biorad, Hercules, CA) in 1x running buffer (29 mM Tris, 144 mM glycine, 1% SDS in water). The gel was transferred to a polyvinylidene difluoride (PVDF) membrane at 100V for one hour in 1x transfer buffer (25mM Tris, 190mM glycine, and 10% methanol). The membrane was blocked with 5% skim milk for one hour and washed 3x with filtered PBST (0.1% Tween 20 (Bioshop Canada Inc, Ontario, Canada) in PBS). The membrane was cut and probed with the glucocorticoid receptor antibody (anti-rabbit, D6H2L; Cell Signalling Biology, Massachusetts, USA), myosin heavy chain (pan MF20 antibody), alpha tubulin antibody (anti-mouse,T5168, Sigma Alderich, Missouri, USA), detyrosinated tubulin antibody (anti-rabbit, ab3201, Millipore Sigma, France), acetylated tubulin antibody (anti-mouse, T7451, Sigma-Aldrich, Missouri, USA), and cyclophilin B (anti-rabbit, ab16045; Abcam, Massachusetts, USA) at 1:1000 concentrations overnight at 4°C. The membrane was washed 3x with PBST and incubated with the appropriate secondary anti-rabbit or anti-mouse specific antibody conjugated with Horseradish Peroxidase (Thermo Fisher, USA) in 1% skim milk in PBST for one hour. The membrane was washed 3x in PBST and detected using enhanced luminol-based chemiluminescent (ECL; Bio-Rad Laboratories, Mississauga, ON) western blotting substrate kit (Bio-Rad Laboratories) at room temperature in the dark for 5 minutes. Chemiluminescence was

detected using the ChemiDoc MP System (Bio-Rad Laboratories), and quantification was analyzed using ImageLab (Bio-Rad Laboratories).

### 2.5 RNA Isolation

Primary myoblast cultures were washed and scraped in PBS and RNA was extracted using RNeasy kit (Qiagen, Toronto, ON). Lysis buffer was added to each sample and homogenized using a BD insulin needle (Fisher Scientific, USA). 70% ethanol was then mixed in by pipetting and the solution was transferred to a RNeasy spin column. RNA was extracted following the manufactures instructions for the kit and RNA extracts eluted in Eppendorf tubes using RNase-free water. The column was centrifuged at 8,000g for one minute to elute the RNA. The optical density of the samples to confirm purity and concentration were measured using the NanoDrop 2000 Spectrophotometer (Thermo Scientific, Wilmington, DE).

### 2.6 RNA-Sequencing Sample Preparation and Analysis

RNA was extracted from myoblasts isolated from WT and $GR^{MUSC-/-}$ mice as described previously in sub-section 2.5. The optical density of the samples was used to confirm purity and concentration were measured using the NanoDrop 2000 Spectrophotometer (Thermo Scientific, Wilmington, DE). Library preparation and sequencing was performed by Genome Quebec. Reads were mapped and aligned to the mouse genome (mm10) using HISAT2, and transcript assembly was guided by stringTie (genecode.vM25.annnotation).

### 2.7 Data Visualization and Analysis

Data and statistical analysis were performed on GraphPad Prism Software (version 10.0.2). When comparing experimental conditions with a control, a two-tailed t-test was used to determine significance (*$p<0.05$, **$p<0.01$). All experiments have a minimum of three biological replicates. Figures are shown as the means of all trials ± standard deviation. When

three or more time points were compared, significance was determined using a one-way analysis of variance (ANOVA). The number of projections per cell was calculated by counting the number of elongated projections from the center body of the cell. The nuclear distance to the cell edge was found using Fiji by measuring the distance from the center of the nucleus to the short edge of the cell on the farthest side. Similarly, the diameter of the short edge of the cells were measured using Fiji. The number of centrally located Golgi elements and centrosomes were quantified by counting those that were found halfway over the nucleus. All cell quantifications were performed on at least 50 cells per condition in triplicates.

## 3. RESULTS

### 3.1 Loss of GR expression in differentiating myoblasts results in abnormal myonuclei placement.

The loss of GR expression results in rounded myotubes[73]. Given that MTs are an essential regulator of both myotube architecture and myonuclear placement, I looked to analyze any nuclear placement defects among WT and $GR^{MuSC-/-}$ myotubes. First, I calculated the internuclear distance defined as the average myotube length divided by the number of nuclei within the myotube (Fig. 4A). We observed a ~48% decrease in the internuclear distance in $GR^{MuSC-/-}$ myotubes as compared to WT samples (Fig. 4B), consistent with rounded cells shape with clumped nuclei observed by Rajgara et al., and by my immunofluorescence staining for MyHC after 24 hours of differentiation (Fig. 4A). The percentage of myotubes where nuclei fail to align along the center of the long axis of the myotube was also quantified (Fig. 4C). $GR^{MuSC-/-}$ myotubes had significantly more myotubes where myonuclei failed to align along the center of the cell when compared to WT cells (37% vs 15%), indicating that GR regulates the alignment phase of myonuclear placement (Fig. 4C). Next, we quantified the number of myotubes with ≥5 clustered nuclei within the myotube (Fig. 4D). This revealed that ~46% of $GR^{MuSC-/-}$ myotubes had clusters of ≥5 nuclei when compared to WT myotubes (~10%) (Fig. 4D). Thus, there is a clear decrease in the average length of myotube per nuclei when GR is lost, indicating that GR plays a role in the overall architecture of the myotubes, including the misalignment and clustering of nuclei.

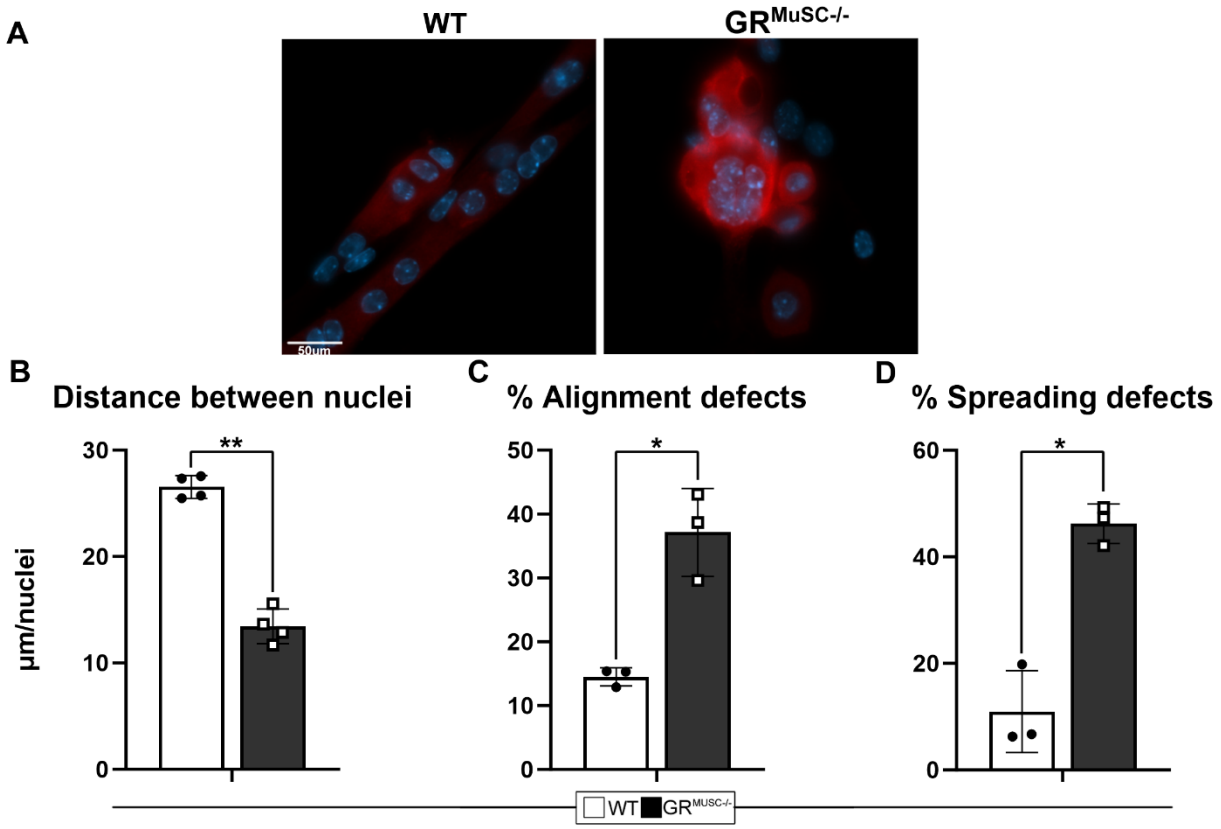


**Figure 4. Loss of GR expression in differentiating myoblasts results in abnormal myonuclei placement.** Isolated muscle stem cells from $GR^{MuSC}$ (*Nr3c1*$^{fl/fl}$ *Pax7*$^{CreER/+}$) and WT (*Nr3c1*$^{fl/fl}$*Pax7*$^{+/+}$) mice that were treated with tamoxifen dissolved in corn oil by i.p. injections for 5 days to induce a knockout of GR were collected by MACS isolation and differentiated for 48 hours. GR expression was verified by western blot. **(A)** Immunofluorescence stain for MyHC and DAPI after 4 hours of differentiation. **(B)** Average distance between nuclei was calculated by the average length of myotubes per number of nuclei within the myotube. n=4 biological replicates **(C)** Percent of myotubes with alignment defects calculated by the number of nuclei that do not align along the center long axis per myotube. **(D)** Percent of myotubes with nuclei accumulated in clumps at extremities of the myotube. n=3 biological replicates $^{*}p<0.05$, $^{**}p<0.005$.

### 3.2 DEX treatment results in star-shaped cells and nuclei localized to one side.

DEX treatment alters the overall morphology of myotubes, resulting in larger cell size with multiple elongated projections that distort the cell shape. Given that MTs are essential regulators of cell shape and architecture, I observed the effects of DEX treatment on the microtubule network[18]. C2C12 cells were cultured in the continuous presence of 1µM DEX or vehicle (ethanol) for up to 48 hours in growth media (GM) to grow and maintain the proliferative state of myoblasts.

Once confluent, C2C12 cells were differentiated for 48 hours (differentiation media, DM) into myotubes. Cells were then stained for detyrosinated tubulin, acetylated tubulin, and DAPI at 24 and 48 hours in GM, and 6, 24, and 48 hours in DM (GM1, GM2, D0+6, D1, D2) (Fig. 5A). When comparing the morphology of DEX treated cells to vehicle, we observed nuclei positioned at the outer edges of the cell during GM2 (Fig. 5A, white arrowheads), and star-like projections emanating from the main body of the cells (Fig. 5A, transparent arrowheads) in DEX treated samples (Fig. 5A). Vehicle treated samples we observe an expected more elongated, lateral cell shape with two distinct poles rather than multiple projections (Fig. 5A). We quantified the number of projections emanating from the main body of the cells and found a significant increase (~50-75%) in the number of projections in DEX treated samples in the GM1, D0+6, D1, and D2 time points when compared to vehicle (Fig. 5B).

We also investigated length from the center of the nucleus to the short edge of the cell to see if there was a significant difference in the placement of the nucleus within the cells. We found an increase in the length from the center of nuclei to the short edge of the cell at GM2 and an increase the diameter of the cells in D0+6h DEX treated samples compared to controls, indicating that the nuclei are pushed further to one side of the cell at these time points (Fig. 5C). However, there is no significant difference in the diameter of the short edge of the cell or the placement of the nuclei within the cell during GM1, D1, or D2 (Fig. 5D, E). These results indicate a change in the overall structure of the cytoskeletal network to create myoblasts and myotubes with star-like projections *in vitro* with DEX treatment, particularly in early differentiation.

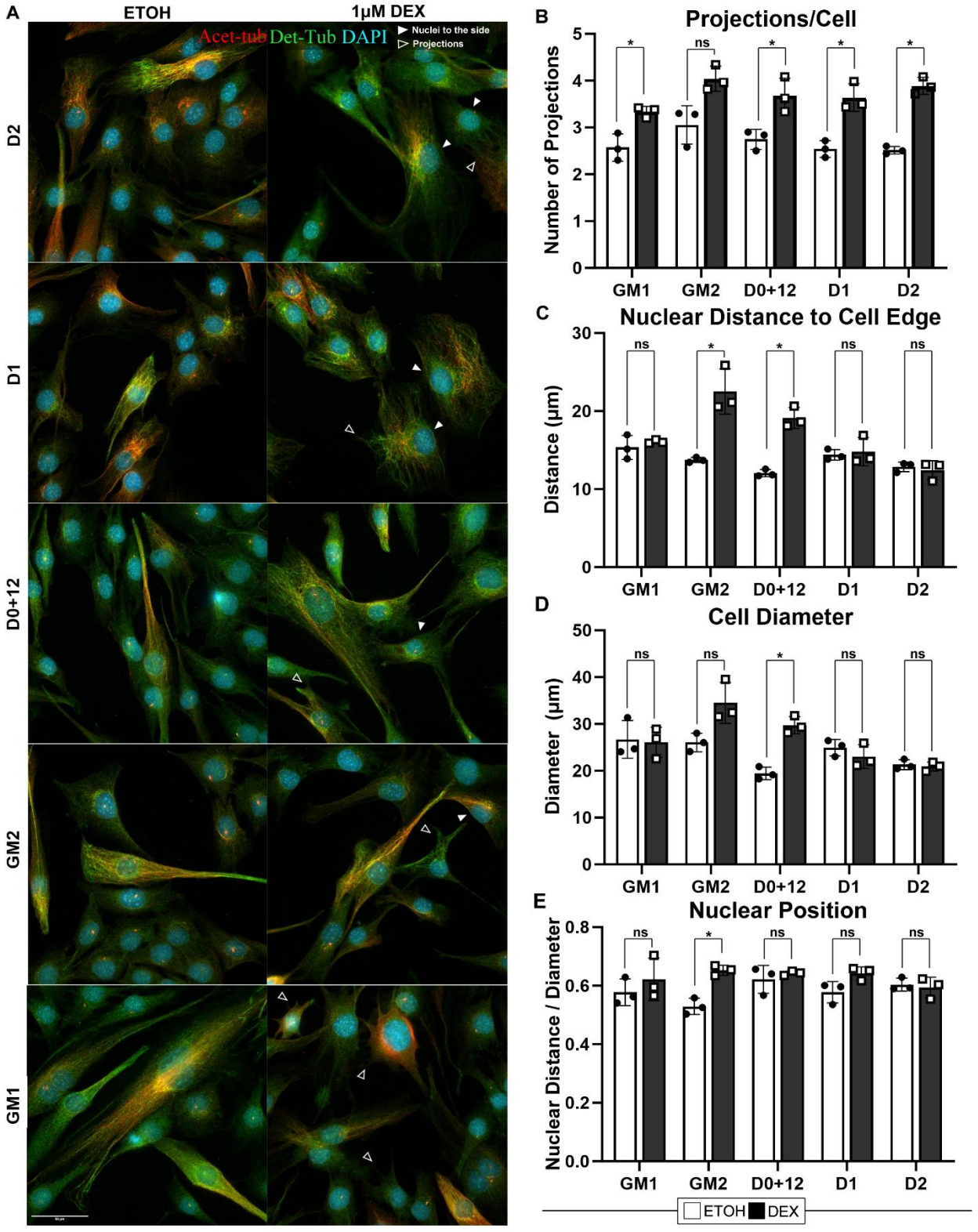


**Figure 5. DEX treatment results in star-shaped cells and nuclei localized to one side. (A)** C2C12 cells were plated in a 6 well plate and grown in either the continuous presence of 1μM DEX or vehicle for 24, 48 hours in GM (GM1, GM2) and 12, 24, and 48 hours in DM (D0+12H, D1, D2) before fixation in paraformaldehyde (PFA). They were immunostained for detyrosinated tubulin (Det-tubulin, green),

acetylated tubulin (Acet-tubulin, red), and nuclei (DAPI). **(B)** Quantification of the number of projections per cell, **(C)** nuclear distance to the short edge of the cells, **(D)** The diameter of the short edge of the cells, and **(E)** the nuclear distance to the short edge of the cells/the diameter of the short edge of the cells for a minimum of 50 cells per time point per treatment. Error bars are ± standard deviation, $^{*}p<0.05$ n=3 pairs. One way analysis of variance (ANOVA) revealed no significant variance in means across time points. $^{****}p<0.0001$.

### 3.3 DEX treatment causes an increase in acetylated tubulin and detyrosinated tubulin levels upon differentiation.

Given that DEX treatment altered the overall structure of myoblasts and myotubes, we further analyzed the effects of DEX on the cytoskeletal network by measuring the intensity of fluorescence of detyrosinated and acetylated tubulin in GM1, GM2, D0+6, D1, and D2 when compared to vehicle (Fig. 6). Both detyrosinated tubulin and acetylated tubulin are PTMs that stabilize the cytoskeletal network and changes in the expression of these PTMs may regulate the ability of muscles to resist contraction forces without breakage and damage. Throughout 48 hours in the proliferative state and 12 hours in differentiation, there was no significant difference in fluorescence intensity of detyrosinated or acetylated tubulin levels per cell in DEX treated samples when compared to vehicle (Fig. 6A, B). However, after 24 and 48 hours in differentiation, there was a significant increase in both detyrosinated and acetylated fluorescence intensity levels per cell in DEX-treated samples compared to vehicle (Fig. 6A, B). This indicates that DEX treatment increases the amount of detyrosinated and acetylated tubulin levels of the cytoskeletal network in early differentiation *in vitro*.

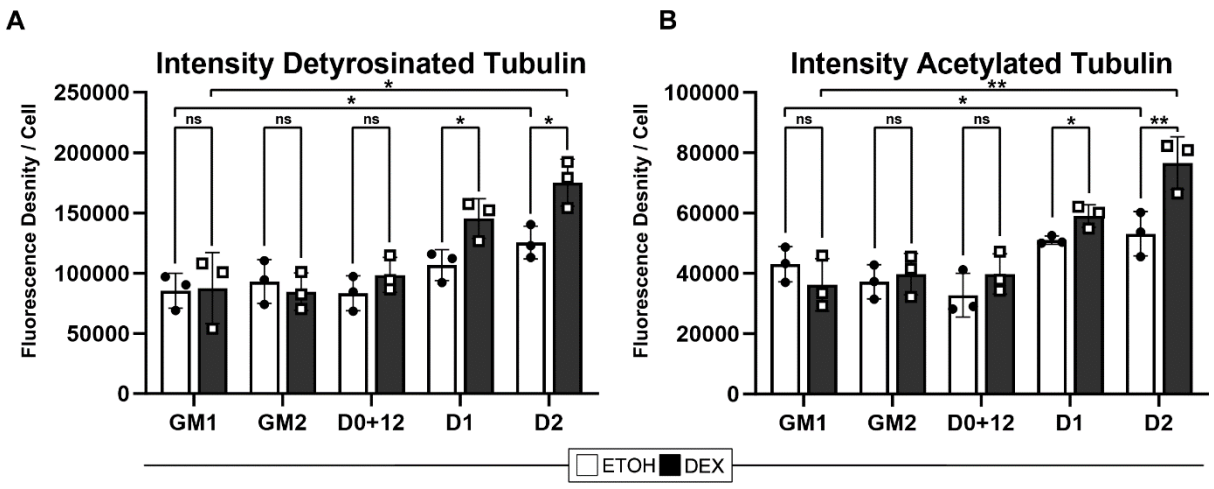


**Figure 6. DEX treatment results in an increase of acetylated tubulin and detyrosinated tubulin levels upon differentiation. (A)** C2C12 cells from Figure 5 were analyzed using Fiji for fluorescence intensity per cell of detyrosinated tubulin staining and **(B)** Acetylated tubulin staining for a minimum of 50 cells per time point per treatment. Error bars are ± standard deviation, $^{*}p<0.05$, $^{**}p<0.005$ n=3 pairs. One way analysis of variance (ANOVA) revealed a significant increase in fluorescence intensity from GM1 to D2.

### 3.4 DEX treatment results in altered Golgi and centrosome placement.

Given that MTOCs are essential for the proper positioning and function of the MT network, I characterized DEX-dependent effects on the Golgi complex and the centrosome. I cultured C2C12 cells in the presence of 1µM DEX or vehicle in GM over a time course of 24 and 48 hours, as well as in DM for 6, 24, 48, and 72 hours and immunostained cells for the Golgi complex, centrosome, and nuclei (Fig. 7A). Under typical conditions, the centrosome and the Golgi complex are located around the periphery of the nucleus. In our samples, the Golgi and centrosome remain in their typical placement at the periphery of the nuclei in both vehicle and DEX treated samples during growth and proliferation (Fig. 7A, B). However, once induced to differentiate, the centrosome and the Golgi complex became centrally located over the apex of the nucleus in DEX-treated samples, while vehicle treated cells remained at the outer edge of the nucleus (Fig. 7A, B, C). We observed a ~18-fold increase in centrally located centrosomes in DEX treated samples after induced to differentiate for 24 hours compared to vehicle, with a total of ~72% of DEX treated

cells having centrally located centrosomes. (Fig. 7B). Similarly, we found a ~8.3-fold increase in central Golgi placement in DEX treated samples at D1 compared to vehicle, with ~49% of total DEX treated cells having centrally located Golgi (Fig. 7C). This data suggests that DEX treatment causes the Golgi and centrosome to misalign from the periphery of the nucleus to the center and that the morphological changes we see in myotubes treated with DEX is an early differentiation defect that persists as myoblasts differentiate.

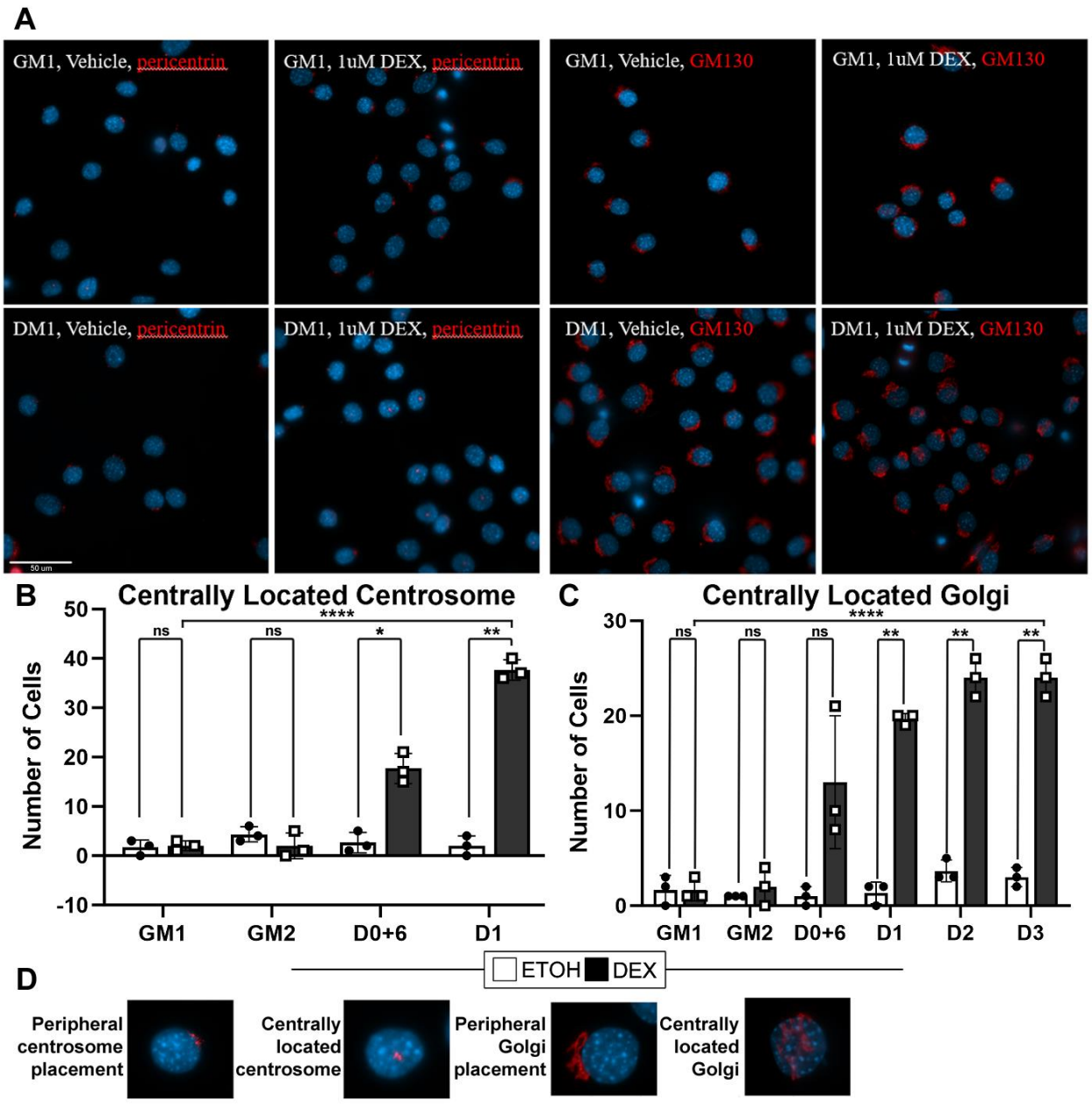

**Figure 7. DEX treatment results in altered Golgi and centrosome placement. (A)** C2C12 cells were plated in a 6 well plate and grown in either the continuous presence of 1μM DEX or vehicle in growth media (GM) for 24 (GM1), and 48 (GM2) hours and then in differentiation media for 6 (D0+6), 24 (D1), 48 (D2), and 72 (D3) hours. Cells were then fixed with PFA and immunostained for the centrosome (pericentrin), Golgi complex (GM13), and the nuclei (DAPI). **(B)** C2C12 cells from (A) were analyzed by counting the centrosomes and **(C)** Golgi that were centrally located on the nucleus compared to normally located centrosome and Golgi on the periphery of the nucleus. 1-way ANOVA analysis showed a significant increase in centrally located Golgi and Centrosome in DEX treated samples from GM to DM **(D)** A representative image of an example of the criteria that we considered centrally located compared to normal placement. Error bars are ± standard deviation n=3, $^{*}p<0.05$, $^{**}p<0.005$. $^{****}p<0.0001$.

### 3.5 Altered Golgi placement in DEX treated myotubes is a GR-dependent phenomenon.

Next, given that GCs regulate multiple mechanisms, I investigated the positioning of the Golgi complex on proliferating and differentiating myoblasts lacking the GR to confirm that the MTOC mispositioning observed previously is due to GCs acting through the GR to produce this phenotype. To produce cells lacking GR, I isolated primary myoblasts from previously generated WT and $GR^{MuSC-/-}$ by magnetic activated cell sorting (MACS). An immunoblot was performed to confirm the knockout of GR expression (Fig. 8A). We observed mispositioning of the Golgi complex in ~50-60% of our WT samples and in ~8-10% of $GR^{MuSC-/-}$ myoblasts with DEX treatment (Fig. 8B). This suggests that misalignment of the Golgi complex over the center of the nucleus is dependent on GCs acting through the GR, as we do not see this effect in muscle cells that lack the GR. Furthermore, this also confirms that the mispositioning of this MTOC occurs in early differentiation and persists throughout later differentiation.

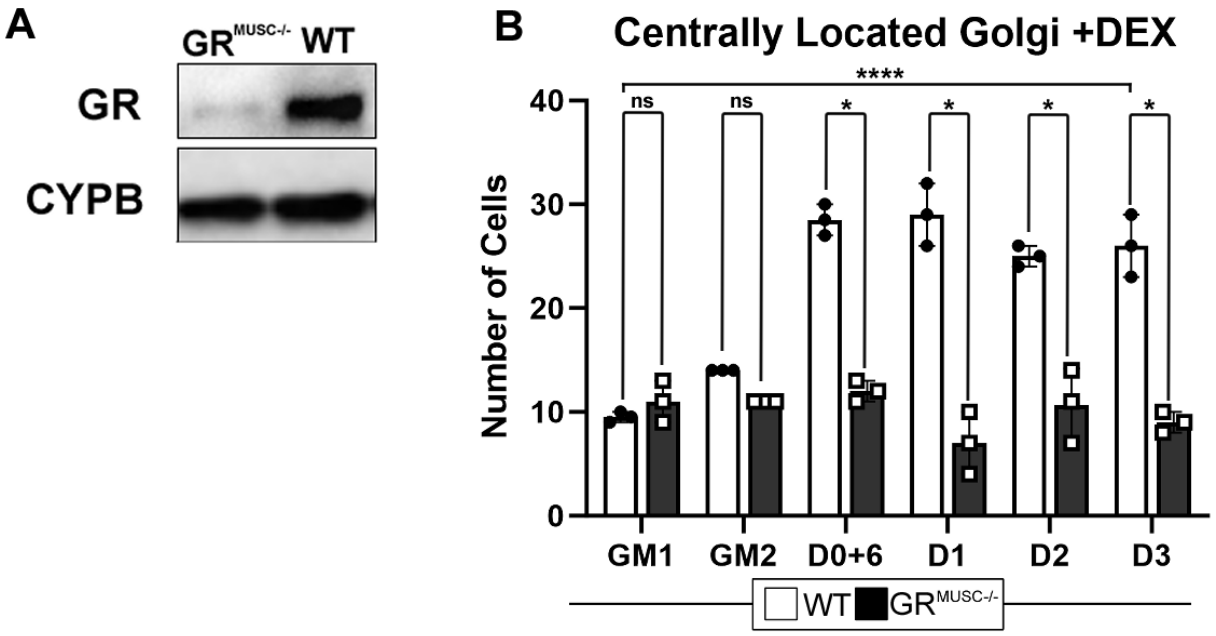


**Figure 8. Altered Golgi placement in DEX treated myotubes is GR dependent.** Myoblasts isolated from *Nr3c1*$^{fl/fl}$*Pax7*$^{CreER/+}$ and *Nr3c1*$^{fl/fl}$*Pax7*$^{+/+}$ mice that were treated with tamoxifen dissolved in corn oil by i.p. injections for 5 days to induce a knockout of GR were collected by MACS isolation and grown. **(A)** Knockdown of the GR was confirmed by western blot. **(B)** Myoblasts were plated and stained as in Figure 9A, and Golgi localization was quantified. Error bars are ± standard deviation n=3 biological replicate pairs, $^{*}p<0.05$, $^{**}p<0.005$.

### 3.6 DEX treatment increases myosin heavy chain and detyrosinated tubulin expression in differentiating myoblasts.

To understand how protein expression is regulated during myoblast differentiation with DEX treatment, C2C12 cells were grown for 48 hours in the continuous presence of 1μM DEX or vehicle, and an additional 48 hours in differentiation media under the same conditions before collection. An immunoblot was performed to assess the relative expression of GR, acetylated tubulin, detyrosinated tubulin, α-tubulin, and myosin heavy chain (MyHC) (Fig. 9A). GR expression is highest in proliferating myoblasts and becomes rapidly downregulated with the onset of differentiation in DEX treated and vehicle samples (Fig. 9A, B). Therefore, the effects on myoblast differentiation from GCs acting through the GR likely occurs during late myoblast proliferation and early differentiation. As expected, myosin heavy chain expression increases as

cells differentiate in both samples, but to a much higher degree in DEX treated cells (~4.94-fold) in comparison to vehicle (Fig. 9C). This is consistent with data from Belanto et al., where DEX was found to increase the synthesis rate of MyHC in skeletal muscles[74]. α-tubulin expression remains relatively stable through proliferation and differentiation with a slight decrease in differentiated cells (Fig. 9D). Meanwhile, both acetylated tubulin and detyrosinated tubulin show no significant difference in overall levels between DEX-treated cells and controls (Fig. 9E, F). However, the proportion of α-tubulin that is detyrosinated increases in DEX treated cells after induced to differentiate ~1.27-fold and ~1.17-fold respectively when compared to vehicle (Fig. 11G, H). These results align with the increase in fluorescence intensity of detyrosinated tubulin previously observed in figure 8, confirming that there is an increase in these PTM levels in DEX treated myoblasts after they were induced to differentiate. Protein expression changes observed in early differentiation further indicates that the initial stages of myoblast differentiation are of particular importance with GC treatment, and that the expression of stabilizing PTMs of MTs like acetylation and detyrosination may play a role in stabilizing the cytoskeletal network with GC treatment.

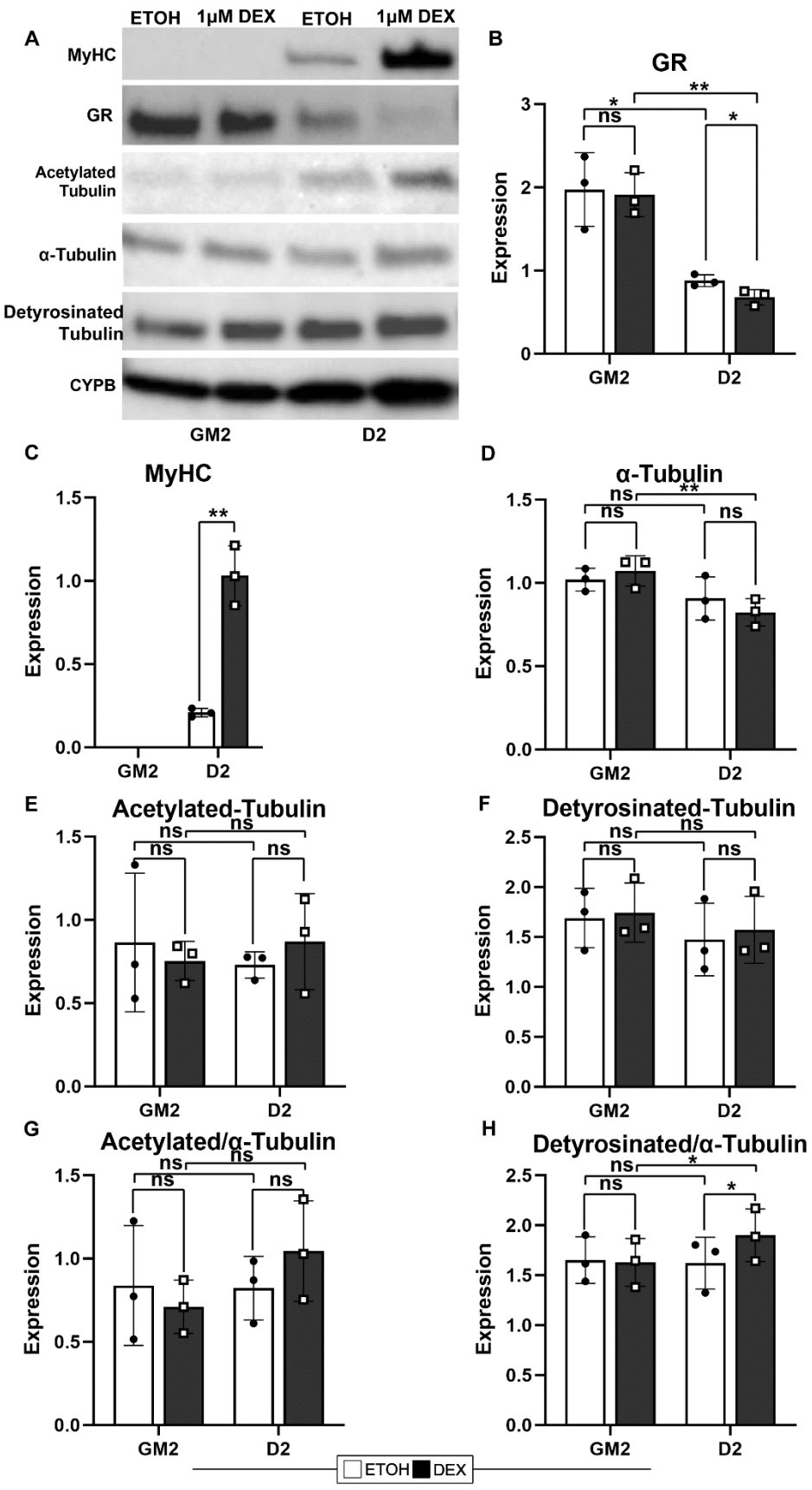
A
ETOH
1μM DEX
ETOH
1μM DEX
MyHC
GR
Acetylated Tubulin
α-Tubulin
Detyrosinated Tubulin
CYPB
GM2
D2
B
GR
Expression
C
MyHC
D
α-Tubulin
E
Acetylated-Tubulin
F
Detyrosinated-Tubulin
G
Acetylated/α-Tubulin
H
Detyrosinated/α-Tubulin
ns
ETOH
DEX

**Figure 9. Protein expression in DEX treated C2C12 myoblasts during differentiation. (A)** C2C12 cells were grown in growth media (GM) in the continuous presence of ethanol (vehicle) or 1μM DEX for 48 hours and collected. A subsequent set of CC12 cells were then switched to differentiation media (DM) for an additional 48 hours in the presence of vehicle or DEX and collected. We performed an immunoblot for the expression of GR, myosin heavy chain (MyHC), acetylated tubulin, α-tubulin, detyrosinated tubulin, and the housekeeping protein cyclophilin B (CYPB). **(B)** Protein expression levels were calculated using band density on Imagelab for GR, **(C)** MyHC, **(D)** α-tubulin, **(E)** acetylated tubulin, **(F)** detyrosinated tubulin, **(G)** acetylated tubulin/ α-tubulin, and **(H)** detyrosinated tubulin/ α-tubulin. Error bars are ± standard deviation n=3 pairs, $^{*}p<0.05$, $^{**}p<0.005$.

### 3.7 Morphological changes in $GR^{MuSC-/-}$ and WT myotubes are not due to differentially expressed genes.

Given that GCs act through the GR, I investigated differential gene expression from WT and $GR^{MuSC-/-}$ myotubes in early and late differentiation. Primary myoblasts isolated from WT and $GR^{MuSC-/-}$ mice by magnetic activated cell sorting (MACS) were grown to confluence before changing to DM. After 24 (D1) and 72 (D3) hours in DM the myotubes were collected using partial trypsinization to collect myotubes and reduce the number of undifferentiated reserve cells in our samples. RNA isolation was completed on 3 biological trials per time point and sent to Genome Quebec for library preparation and sequencing. A portion of each sample was kept for immunoblotting to confirm the knockout of GR (Fig. 10A). We used Fastp to trim adapters and low-quality sections and reads were aligned to the mouse genome (mm10 assembly) using STAR and an index was created using a gene model GTF file (Mus_musculus.GRCm38.102.gtf, from ENSEMBL). Principal component analysis revealed segregation dependent on time points rather than genotype (Fig. 10B). Consistent with this, a heatmap of the top 2000 genes, sorted by k mean, where k=6 revealed little differences between genotypes at either timepoint (Fig. 10C), though *Nr3c1*, encoding the GR, was reduced in $GR^{MuSC-/-}$ samples compared to WT (Fig. 10D). Therefore, we investigated the differentially expressed genes between genotypes at D3 and D1 (Fig. 10E). This analysis showed 5 downregulated genes (*Nr3c1, Gm2541, Gm28900, Snurf,* and

*Gm47924*) and 2 upregulated genes (*Gm10036,* and *Gm6565*) when comparing $GR^{MuSC-/-}$ and WT samples from D1 (Fig. 10E). *Gm2541* is a predicted pseudogene of DnaJ (Hsp40) that functions in Hsp70 binding. *Gm28900* is a predicted gene with unknown function. *Snurf is* SNRPN upstream reading frame that encodes a protein involved in mRNA splicing and enables ATPase binding. *Gm10036* is a predicted gene for ribosomal protein L11, a ribosomal protein that is a component of the 60S subunit. *Gm6565* is a predicted gene of ubiquitin-conjugating enzyme E2. Additionally, we found 1 downregulated gene (*Nr3c1)* and 3 upregulated genes (*Gm10036, Gm6565, and Gm27029*) when comparing $GR^{MuSC-/-}$ and WT samples from D3 (Fig. 10E). *Gm27029* is a predicted gene that is involved in catalyzing alanine-tRNA ligase activity and ATP binding. Overall, there were very few differentially expressed genes between WT and $GR^{MuSC-/-}$ myotubes at both time points, and the few genes that were found were primarily predicted genes with unknown or poorly understood function. This indicates that despite morphological differences observed previously between WT and $GR^{MuSC-/-}$ myotubes, both have similar gene expression patterns at 24 and 72 hours in differentiation.

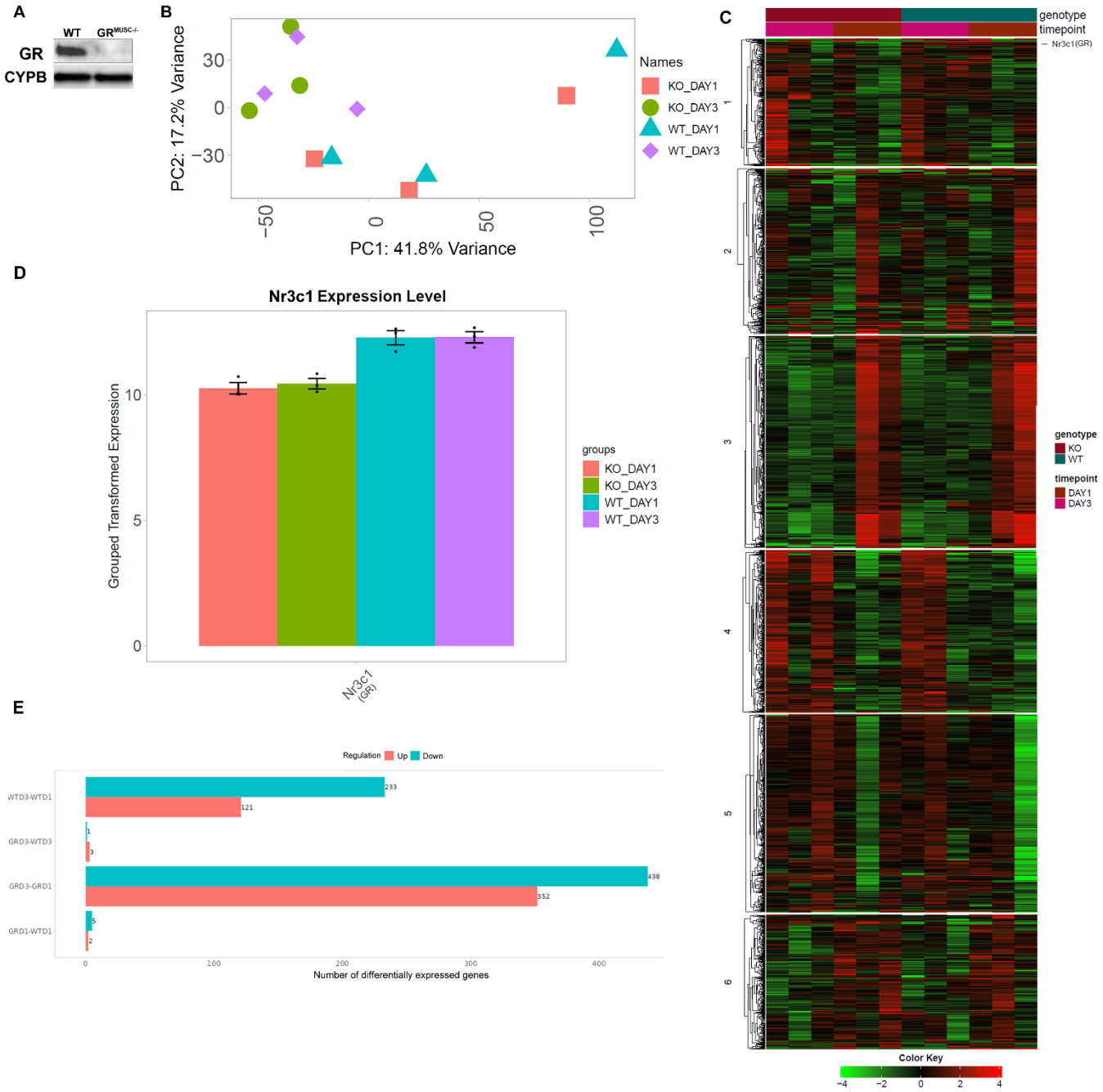


**Figure 10. RNA sequenced from GR$^{MuSC-/-}$ and WT myotubes during stages of early and late differentiation.** Myoblasts isolated from *Nr3c1*$^{fl/fl}$*Pax7*$^{CreER/+}$ and *Nr3c1*$^{fl/fl}$*Pax7*$^{+/+}$ mice that were treated with tamoxifen dissolved in corn oil by i.p. injections for 5 days to induce a knockout of GR were collected by MACS isolation and grown **(A)** Knockdown of the GR was confirmed by western blot. **(B)** Principal Component Analysis plot showing clusters of samples based on their similarity in RNA sequenced from WT and GR$^{MuSC-/-}$ muscle stem cells in differentiation for 24 hours (D1), and 72 hours (D3). **(C)** Heatmap of the top 2000 genes of k means where k=6. **(D)** Grouped transformed expression level of the Nr3c1 gene. **(E)** Number of differentially expressed genes comparing in GR$^{MuSC-/-}$ and WT samples at D1 and D3, false discovery rate cut off=0.05 and a minimum fold change of 1. n=3 biological replicate pairs.

## 4. DISCUSSION

DMD is a severe muscle wasting disease caused by a lack of functional dystrophin which is primarily treated by GCs[52]. Low-dose, short-term treatment with GCs improves symptoms for the first 6 months and stabilizes the disease for up to 3 years, however, long-term treatments reduce muscle function and accelerate disease progression[40]. GCs have many mechanisms of action, and it is still unclear which pathways produce the positive and negative effects we see[39]. This research aims to characterize GC-induced effects on nuclear positioning, MT organization, and MT dynamics in myoblasts and myotubes with DEX treatment to uncover cellular processes that may contribute to these positive and negative effects.

First, we observed the cytoskeletal network of primary myoblasts throughout proliferation and differentiation to describe changes in the morphology and MT stabilizing markers by staining for acetylated and detyrosinated tubulin. These results suggest that DEX treatment of MuSCs causes an increase in the number of cytoskeletal projections as myoblasts are differentiated *in vitro*. The increase in branching of the cytoskeletal network may be one way in which DEX can reduce contraction induced damage on the myofibers by more evenly distributing mechanical forces. This branching effect has been observed in neurons as well, where DEX has been shown to increase dendritic branching and neuronal growth[75]. However, MuSCs grown *in vitro* will not accurately represent a cells morphology *in vivo*. Myofiber growth and regeneration *in vivo* have a scaffold of muscle fibers in place for differentiating myoblasts to adhere to and grow in a specific polar direction, as well as a complex microenvironment consisting of immune cells, fibroblasts, pericytes, etc., that regulate and maintain muscle cell growth and differentiation. *In vitro* experiments of myoblast growth and differentiation are unable to fully replicate this complex environment. However, it would be of interest to observe the cytoskeletal network of MuSCs on a

flex plate to provide the lateral tension that muscle fibers undergo *in vivo*. This may give us a more accurate representation of how this branching effect with DEX treatment may present itself *in vivo*. Another interesting experiment would be to perform live cell imaging of the MTs while bound to the flex plate using a depolymerizing agent like nocodazole to observe in real time any differences DEX treatment may have on morphology and MT regrowth velocity and direction.

Given that the MTOCs are essential for the proper organization and functioning of the MT network, we investigated the effects of DEX treatment on the centrosome and the Golgi apparatus in proliferating and differentiating MuSCs. We observed that both the centrosome and Golgi were located in the perinuclear region in all samples, but once myoblasts were induced to differentiate, the DEX treated samples exhibited a significant number of centrosomes and Golgi complexes located apically over the center of the nucleus. The Golgi apparatus is a major nucleating center for MTs, and the actin and MT network play a key role in maintaining Golgi positioning, architecture, and polarization[16]. As myoblasts differentiate, their Golgi complex is located at the periphery of the nuclear membrane but upon fusion of myotubes into myofibers the Golgi complex is replaced by smaller Golgi elements and the radial MTs emanating from the nucleus reposition to form an orthogonal, parallel network. These Golgi elements in myofibers are typically positioned at the vertices of an orthogonal lattice MT network[16]. Myofibers lacking dystrophin showed randomly placed Golgi elements throughout myofibers that produce a randomly oriented MT network in muscle fibers lacking dystrophin[21] Thus, the anchoring and positioning of Golgi elements that nucleate the MT network regulate the positioning of the cytoskeletal lattice network[21]. Furthermore, MTs originating from the nucleus are stabilized and reach longer distances than those nucleated from Golgi elements in the cytogolplasm[21]. This indicates that the central nuclear positioning of the Golgi and centrosome observed in differentiating myoblasts with

DEX treatment may be caused by a lack of polarity and likely contributes to a more branched, stable MT network that may lead to mispositioning of Golgi elements and perpetuate a branched cytoskeletal network. This idea is supported by Kodani & Sutterlin who found that the Golgi complex regulates the proper positioning of the centrosome, and mispositioning of the MTOC results in nonfunctional multipolar spindles during mitosis[76]. Furthermore, a knockdown in GR is known to cause mitotic spindle defects, including delayed anaphase, ternary chromosome segregation and apoptosis, indicating that the altered positioning observed in DEX treated cells upon differentiation causes mispositioning of the MTOC, likely leading to defects in the MTs that compose the mitotic spindles[76]. Given that the mispositioning of the MTOC is only observed after induction to differentiation, it also suggests that the branched morphological changes we see in myotubes treated with DEX are an early differentiation defect that persists throughout differentiation. The Golgi also plays a key role in the secretory pathway and is responsible for modifying proteins and lipids and sorting molecules to their correct position[77]. Disruption of this pathway between the endoplasmic reticulum and Golgi can result in downstream defects in molecular machinery causing disease[77]. Changes in the morphology and positioning of the Golgi complex has been shown to result in impairment of glycosylation of proteins, and fragmentation of the Golgi complex has been observed in Parkinson's disease, dependent on the expression levels of GTP binding proteins[77]. There are now a significant number of diseases associated with Golgi mispositioning and Golgi proteins, however the precise link between loss of Golgi homeostasis and disease phenotype remains unknown[77]. Therefore, the mispositioning of the Golgi complex observed in differentiation of DEX treated myoblasts may also result in modifications of the secretory pathway and alterations of protein modifications by the Golgi complex.

Furthermore, to confirm our hypothesis that these morphological changes are due to GCs acting through the GR, we conducted the same experiment on WT and $GR^{MuSC-/-}$ myoblasts. GR is related to the mineralocorticoid receptor (MR) that responds to aldosterone to regulate blood pressure[78]. While the main receptor for GCs is GR, the MR can also bind to low cortisol levels with a high affinity[78]. When GR and MR are present, endogenous cortisol preferentially occupies the MR, with GR ligand binding seen at higher levels[79]. GR and MR are both expressed in MuSCs, but MR mRNA is weakly expressed in skeletal muscle, making GR the primary receptor for GCs[79]. Therefore, we looked to confirm that the morphological differences we see in MuSCs with DEX treatment are due to GCs acting through the GR rather than the MR. Our results confirmed that the central placement of the Golgi observed previously in DEX treated samples upon differentiation does not occur in $GR^{MuSC-/-}$ myotubes. This validates that the centrally located MTOC we observed is due to DEX acting through the GR, as $GR^{MuSC-/-}$ cells do not have the GR for GCs to act through. This reiterates that GCs act through the GR in early differentiation to change the placement of the MTOC from the periphery of the nucleus to the center of the nucleus.

The proportion of detyrosinated α-tubulin is significantly higher in DEX treated samples after differentiation with a significant increase in detyrosinated tubulin from GM2 to D2. The immunoblot results validate the immunofluorescent intensity of acetylation and detyrosination levels observed in differentiating myoblasts, where we observed an increase in both acetylation and detyrosination fluorescence intensity in DEX treated myoblasts after induced to differentiate. This further illustrates that we do not see any significant differences in these PTMs in proliferating MuSCs, but upon differentiation with DEX treatment, a higher expression level of detyrosination occurs, indicating an increase in the stability of the MT network of DEX-treated myotubes, likely caused by activating acetyltransferases and carboxypeptidases or by inhibiting deacetylases and

tubulin-tyrosine ligases. This reiterates that early differentiation is an important time point where DEX-treated cells begin to show differences in both morphology and protein levels. Furthermore, we observed a significant increase in the levels of MyHC expression in differentiated myotubes treated with DEX. This coincides with the findings by Belanto et al, where DEX treatment significantly increased MyHC levels, as well as enhanced myogenic fusion efficiency[74]. Myocyte fusion is necessary for effective regeneration of damaged muscle, and increased fusion efficiency and MyHC levels may contribute to more efficient regeneration in dystrophic muscle treated with GCs. Overall, the increase in MT PTM stability markers upon differentiation of DEX-treated myotubes indicates that GCs may increase the stability of the cytoskeleton and increase myogenic fusion in early differentiation to reduce mechanical muscle damage and increase the stability of dystrophic muscles.

Finally, given that GCs act through the GR, we investigated differential gene expression from WT and $GR^{MuSC-/-}$ myotubes in early and late differentiation to uncover any potential gene expression changes that may contribute to GC efficacy. Given the high variability observed in our dataset, there were few differentially expressed genes when comparing $GR^{MuSC-/-}$ and WT samples. I found differential expression in *Nr3c1, Gm2541, Gm28900, Snurf, Gm47924, Gm10036, and Gm6565* when comparing $GR^{MuSC-/-}$ and WT samples from D1, as well as *Nr3c1, Gm10036, Gm6565, and Gm27029* when comparing $GR^{MuSC-/-}$ and WT samples from D3. The majority of these genes are predicted genes or pseudo genes, and none have a described function in the regulation of cell polarity, cell shape, or the cytoskeleton. This suggests that morphological changes in $GR^{MuSC-/-}$ and WT myotubes are not due to differential gene expression at these time points. It is of particular interest to further investigate any differentially expressed genes related to cell polarity, cell shape, and the cytoskeleton, with DEX treatment to observe any potential

changes that may contribute to the stability of the MT network and dispersing contractile forces. However, given the variability in this RNA-seq dataset, an in-depth RNA-seq experiment including DEX and vehicle treated $GR^{MuSC-/-}$ and WT samples is required to uncover any differentially expressed genes between proliferation and differentiation in both genotypes. Early differentiation is shown to be an important time point where DEX treatment exhibits morphological changes in myotubes, and sequencing this data may uncover potential functional gene pathways that contribute to the positive and negative effects of GC use.

## 5. CONCLUSION

DMD is a sever muscle wasting disease caused by the loss of functional dystrophin in 1 in every 3500 births[34]. Paradoxically, the synthetic GC, prednisone, is the standard treatment for DMD, despite the fact that muscle wasting is a common side effect of GCs[52]. Low-dose, short-term prednisone treatment improves symptoms for the first 6 months and stabilizes the disease for up to 3 years, but long-term treatments reduce muscle function and accelerate disease progression[40]. This study provides insight into the specific structural components that are altered by GCs by characterizing the GC induced effects on nuclear positioning, MT organization, and MT dynamics in MuSCs. This research suggests that DEX treatment increases branching of the MT network, increases the MT stabilizing markers acetylated and detyrosinated tubulin, and relocates the Golgi complex from the periphery of the nucleus to the center of the nucleus during early differentiation. This indicates that GCs act through the GR in early differentiation to regulate the cytoskeletal network through changes in PTMs of tubulin subunits and through the reorganization of the MTOC. Thus, GCs are regulators of the MT network, and further in-depth studies to uncover the exact mechanisms of this remodeling and the functional effects is required to better understand how GCs function with short term and long-term use.

## 6. REFRENCES


1. Cornelison, D., & Wold, B. Single-Cell Analysis of Regulatory Gene Expression in Quiescent and Activated Mouse Skeletal Muscle Satellite Cells. *Dev Biol*, **191** (2), 270-283 (1997).
2. Seale, P., Sabourin, L., Girgis-Gabardo, A., Mansouri, A., P. Gruss, P. & Rudnicki M. Pax7 is required for the specification of myogenic satellite cells. *Cell.* **102,** 777-786 (2000).
3. Fukada, S., Uezumi A, Ikemoto M., Masuda, S., Segawa M., Tanimura N., Yamamoto H., Miyagoe-Suzuki Y. & Takeda S. Molecular signature of quiescent satellite cells in adult skeletal muscle. *Stem Cells*, **25** (10), 2448–59 (2007).
4. Kuang, S., Kuroda, K., Le Grand, F. & Rudnicki, M. Asymmetric Self-Renewal and Commitment of Satellite Stem Cells in Muscle. *Cell*, **129**, 999–1010 (2007).
5. Gnocchi, V., White, R., Ono, Y., Ellis, J. & Zammit, P. Further characterization of the molecular signature of quiescent and activated mouse muscle satellite cells. *PloS one*, **4** (4), p.e 5205 (2009).
6. Yin, H., Price, F. & Rudnicki, M. a. Satellite cells and the muscle stem cell niche. Physiol. Rev. 93, 23–67 (2013).
7. Seale, P. et al. Pax7 is necessary and sufficient for the myogenic specification of CD45+:Sca1+stem cells from injured muscle. PLoS Biol 2, E130 (2004).
8. Irintchev, A., Zeschnigk, M., Starzinski-Powitz, A. & Wernig, A. Expression pattern of Mcadherin in normal, denervated, and regenerating mouse muscles. Dev. Dyn. 199, 326–337 (1994).
9. Cornelison, D. D., Filla, M. S., Stanley, H. M., Rapraeger, a C. & Olwin, B. B. Syndecan-3 and syndecan-4 specifically mark skeletal muscle satellite cells and are implicated in satellite cell maintenance and muscle regeneration. Dev. Biol. 239, 79–94 (2001).
10. Ratajczak, M. et al. Expression of functional CXCR4 by muscle satellite cells and secretion of SDF-1 by muscle-derived fibroblasts is associated with the presence of both muscle progenitorsin bone marrow and hematopoietic stem/progenitor cells in muscle. Stem Cells 21, 363–371 (2003).
11. Hernández-Hernández JM, García-González EG, Brun CE, Rudnicki MA. *The myogenic regulatory factors, determinants of muscle development, cell identity and regeneration.* Semin Cell Dev Biol. 2017 Dec;72:10-18. doi: 10.1016/j.semcdb.2017.11.010. Epub 2017 Nov 15. PMID: 29127045; PMCID: PMC5723221.
12. Megeney, L. A., Kablar, B., Garrett, K., Anderson, J. E. & Rudnicki, M. A. MyoD is required for myogenic stem cell function in adult skeletal muscle. Genes Dev 10, 1173–1183 (1996).
13. Hasty, P.,Bradley, A., Morris, J., Edmondson, D., Venuti, J., Olson, E. & Klein, W. Muscle deficiency and neonatal death in mice with a targeted mutation in the myogenin gene. *Nature*, **364** (6437), 501–506 (1993).
14. Chen, J. & Goldhamer, D. Transcriptional mechanisms regulating MyoD expression in the mouse. *Cell tissue res*, **296**(1), 213–9 (1999).

15. Tedesco, F., Dellavalle, A., Diaz-Manera, J., Messina, G. & Cossu, G. Repairing skeletal muscle: regenerative potential of skeletal muscle stem cells. *J Clin Invest*, **120**(1), 11–19 (2010).
16. Oddoux, S. et al. Microtubules that form the stationary lattice of muscle fibers are dynamic and nucleated at golgi elements. *J. Cell Biol.*, **203**, 205–213 (2013).
17. Cadot, B., Gache V., & Gomes, E. Moving and positioning the nucleus in skeletal muscle – one step at a time, *Nucleus*, **6** (5), 373-381 (2015).
18. Brouhard, G. J. & Rice, L. M. Microtubule dynamics: An interplay of biochemistry and mechanics. Nature Reviews Molecular Cell Biology vol. 19 451–463 (2018).
19. Becker R, Leone M, Engel FB. *Microtubule Organization in Striated Muscle Cells*. Cells. 2020 Jun 3;9(6):1395. doi: 10.3390/cells9061395. PMID: 32503326; PMCID: PMC7349303.
20. Wloga, D., Joachimiak, E. & Fabczak, H. Tubulin post-translational modifications and microtubule dynamics. *Intl J. Mol Sci*, 18 (2017).
21. Oddoux, S. et al. Misplaced Golgi Elements Produce Randomly Oriented Microtubules and Aberrant Cortical Arrays of Microtubules in Dystrophic Skeletal Muscle Fibers. *Front. Cell Dev. Biol*. **7**, (2019).
22. Cadot, B., Gache, V., Vasyutina, E., Falcone, S., Birchmeier, C., Gomes E. Nuclear movement during myotube formation is microtubule and dynein dependent and is regulated by Cdc42, Par6 and Par3. *EMBO Rep*, **13**:741-749 (2012).
23. Espigat-Georger, A., Dyachuk, V., Chemin, C., Emorine, L., Merdes, A. Nuclear alignment in myotubes requires centrosome proteins recruited by nesprin-1. *Journal of Cell Science*, **129**: 4227-4237 (2016).
24. Metzger, T., Gache, V., Xu, M., Cadot, B., Folker, E., Richardson, B., Gomes, E., Baylies M. MAP and Kinesin dependent nuclear positioning is required for skeletal muscle function. *Nature*. **484**(7392): 120–124 (2012).
25. Wilson, M., Holzbaur, E. Nesprins anchor kinesin-1 motors to the nucleus to drive nuclear distribution in muscle cells. *Development*, **142**(1):218–228 (2015).
26. Olaia F. et al. Bioengineered optogenetic model of human neuromuscular junction, Bioomaterials, Vol. 276, 2021. Doi.org/10.1016/j.biomaterials.2021.121033.
27. Janin A, Gache V. Nesprins and Lamins in Health and Diseases of Cardiac and Skeletal Muscles. Front Physiol. 2018 Sep 7;9:1277. doi: 10.3389/fphys.2018.01277. PMID: 30245638; PMCID: PMC6137955.
28. Srsen, V., Fant, X., Heald, R., Rabouille, C., Merdes, A. Centrosome proteins form an insoluble perinuclear matrix during muscle cell differentiation, *BMC Cell Biol*. **10**, 28 (2009).
29. Tassin, A., Maro, B., Bornens, M. Fate of microtubule-organizing centers during myogenesis in vitro. *J. Cell Biol.* **100**, 35–46 (1985).
30. Roll-Mecak, A. The Tubulin Code in Microtubule Dynamics and Information Encoding. Developmental Cell vol. 54 7–20 (2020).
31. Gundersen GG, Khawaja S, Bulinski JC. *Generation of a stable, posttranslationally modified microtubule array is an early event in myogenic differentiation.* J Cell Biol. 1989

Nov;109(5):2275-88. doi: 10.1083/jcb.109.5.2275. PMID: 2681230; PMCID: PMC2115884.
32. Zhang Y, Li N, Caron C, Matthias G, Hess D, Khochbin S, Matthias P. *HDAC-6 interacts with and deacetylates tubulin and microtubules in vivo*. EMBO J. 2003 Mar 3;22(5):1168-79. doi: 10.1093/emboj/cdg115. PMID: 12606581; PMCID: PMC150348.
33. Hoffman E.P., Brown R. H., Jr, & Kunkel L., M. Dystrophin: The protein product of the Duchenne muscular dystrophy locus. *Cell* **51**(6): 919–928 (1987).
34. Petrof, B. J., Shrager, J. B., Stedman, H. H., Kelly, A. M. & Sweeney, H. L. Dystrophin protects the sarcolemma from stresses developed during muscle contraction. *Proc. Natl. Acad. Sci. U. S. A.* **90,** 3710–3714 (1993)
35. Gao QQ, McNally EM. *The Dystrophin Complex: Structure, Function, and Implications for Therapy*. Compr Physiol. 2015 Jul 1;5(3):1223-39. doi: 10.1002/cphy.c140048. PMID: 26140716; PMCID: PMC4767260.
36. Dellorusso, C., Crawford, R. W., Chamberlain, J. S. & Brooks, S. V. Tibialis anterior muscles in mdx mice are highly susceptible to contraction-induced injury. *J. Muscle Res. Cell Motil.* **22,** 467–475 (2001).
37. Moens, P., Baatsen, P. H. W. W. & Maréchal, G. Increased susceptibility of EDL muscles from mdx mice to damage induced by contractions with stretch. *J. Muscle Res. Cell Motil.* **14,** 446–451 (1993).
38. Dumont, N. A. *et al.* Dystrophin expression in muscle stem cells regulates their polarity and asymmetric division. *Nat. Med.* **21,** 1455–1463 (2015).
39. Miyatake, S., Shimizu-Motohashi, Y., Takeda, S. & Aoki, Y. Anti-inflammatory drugs for Duchenne muscular dystrophy: focus on skeletal muscle-releasing factors. *Drug Design, Development and Therapy* **10**, 2745–2758 (2016).
40. Drachman D.B., Toyka K.V. & Myer E. Prednisone in Duchenne muscular dystrophy. *Lancet* **2**(7894): 1409–1412 (1974).
41. Mendell J.R., *et al*. Randomized, double blind six-month trial of prednisone in Duchenne's muscular dystrophy. *N Engl J Med* **320**(24): 1592–1597 (1989).
42. Bodine, S. C. & Furlow, J. D. Glucocorticoids and skeletal muscle. *Adv. Exp. Med. Biol.* **872**, 145–176 (2015).
43. Quattrocelli, M. et al. Intermittent glucocorticoid steroid dosing enhances muscle repair without eliciting muscle atrophy. J. Clin. Invest. 127, 2418–2432 (2017).
44. Salamone IM, Quattrocelli M, Barefield DY, Page PG, Tahtah I, Hadhazy M, Tomar G, McNally EM. *Intermittent glucocorticoid treatment enhances skeletal muscle performance through sexually dimorphic mechanisms*. J Clin Invest. 2022 Mar 15;132(6):e149828. doi: 10.1172/JCI149828. PMID: 35143417; PMCID: PMC8920338.
45. Sklar, R. M. & Brown, R. H. J. Methylprednisolone increases dystrophin levels by inhibiting myotube death during myogenesis of normal human muscle in vitro. *J. Neurol. Sci.* **101**, 73–81 (1991).
46. Pasquini, F. *et al*. The effect of glucocorticoids on the accumulation of utrophin by cultured

normal and dystrophic human skeletal muscle satellite cells. *Neuromuscul. Disord.* **5**, 105–114 (1995).
47. Rhen T. & Cidlowski J. A. Anti- inflammatory action of glucocorticoids- new mechanisms for old drugs. *N Engl J Med.* **353**:1711-1723 (2005).
48. Ramamoorthy, S. & Cidlowski, J. A. Corticosteroids: Mechanisms of Action in Health and Disease. *Rheum. Dis. Clin. North Am.* **42**, 15–31, vii (2016).
49. Barshes NR, Goodpastor SE, Goss JA. *Pharmacologic immunosuppression.* Front Biosci. 2004 Jan 1;9:411-20. doi: 10.2741/1249. PMID: 14766378.
50. Shepherd, S., Batra, A. & Lerner, D. P. Review of Critical Illness Myopathy and Neuropathy. The Neurohospitalist 7, 41–48 (2017).
51. Yang R, Yu Y. *Glucocorticoids are double-edged sword in the treatment of COVID-19 and cancers.* Int J Biol Sci. 2021 Apr 10;17(6):1530-1537. doi: 10.7150/ijbs.58695. PMID: 33907516; PMCID: PMC8071771.
52. Mcdonald, C. M. et al. Long-term effects of glucocorticoids on function, quality of life, and survival in patients with Duchenne muscular dystrophy: a prospective cohort study. Lancet 391, 451–461 (2018).
53. Kumar, R. & Thompson, E. Gene regulation by the glucocorticoid receptor: structure: function relationship. *J Steroid Biochem Mol Biol,* **94**:383–94 (2005).
54. Grad I. & Picard D. The glucocorticoid responses are shaped by molecular chaperones. *Mol Cell Endocrinol*. **275**:2–12 (2007).
55. Pratt W.B., & Toft D.O. Steroid receptor interactions with heat shock protein and immunophilin chaperones. *Endocr Rev*. **18**:306–60 (1997).
56. Moras, D. & Gronemeyer, H. The nuclear receptor ligand-binding domain: structure and function. *Curr. Opin. Cell Biol*. **10**, 384–391 (1998).
57. Guiochon-Mantel, A. *et al*. Mechanisms of nuclear localization of the progesterone receptor. *J. Steroid Biochem. Mol. Biol*. **41**, 209–215 (1992).
58. Karin M, Chang L. AP-1-glucocorticoid receptor crosstalk taken to a higher level. J Endocrinol 2001; 169:447-451
59. Barnes PJ, Karin M. Nuclear factor-kB: a pivotal transcription factor in chronic inflammatory diseases. N Engl J Med 1997; 336:1066-1071
60. Didonato JA, Saatcioglu F, Karin M. Molecular mechanisms of immunosuppression and anti-inflammatory activities by glucocorticoids. Am J Respir Crit Care Med 1996; 154:S11-15
61. Kino T. Glucocorticoid Receptor. [Updated 2017 Aug 15]. In: Feingold KR, Anawalt B, Boyce A, et al., editors. Endotext [Internet]. South Dartmouth (MA): MDText.com, Inc.; 2000-. Available from: https://www.ncbi.nlm.nih.gov/books/NBK279171/
62. Reichardt, H.M. *et al*. Glucocorticoid signalling-multiple variations of a common theme. *Mol Cell Endocrinol.* **146**(1-2): 1-6 (1998).
63. Wiper-Bergeron, N., Salem, H. A., Tomlinson, J. J., Wu, D. & Haché, R. J. G. Glucocorticoid-stimulated preadipocyte differentiation is mediated through acetylation of

C/EBPbeta by GCN5. *Proc. Natl. Acad. Sci. U. S. A.* **104,** 2703–2708 (2007).
64. Wiper-Bergeron, N., Wu, D., Pope, L., Schild-Poulter, C. & Haché, R. J. G. Stimulation of preadipocyte differentiation by steroid through targeting of an HDAC1 complex. *EMBO J.* **22,** 2135–2145 (2003).
65. Alamdari, N., Aversa, Z., Castillero, E. & Hasselgren, P. O. Acetylation and deacetylation - Novel factors in muscle wasting. Metabolism: Clinical and Experimental vol. 62 1–11 (2013).
66. Kershaw, S. et al. Glucocorticoids rapidly inhibit cell migration through a novel, non-Transcriptional HDAC6 pathway. J. Cell Sci. 133, (2020).
67. Akner, G. et al. Glucocorticoid receptor inhibits microtubule assembly in vitro. Mol. Cell. Endocrinol. 110, 49–54 (1995).
68. Rovito D, Rerra AI, Ueberschlag-Pitiot V, Joshi S, Karasu N, Dacleu-Siewe V, Rayana KB, Ghaibour K, Parisotto M, Ferry A, Jelinsky SA, Laverny G, Klaholz BP, Sexton T, Billas IML, Duteil D, Metzger D. *Myod1 and GR coordinate myofiber-specific transcriptional enhancers. Nucleic Acids Res.* 2021 May 7;49(8):4472-4492. doi: 10.1093/nar/gkab226. PMID: 33836079; PMCID: PMC8096230.
69. Matthews LC, Berry AA, Morgan DJ, Poolman TM, Bauer K, Kramer F, et al. Glucocorticoid receptor regulates accurate chromosome segregation and is associated with malignancy. Proc Natl Acad Sci U S A. 2015;112(17):5479–84.
70. Matthews LC, Berry AA, Morgan DJ, Poolman TM, Bauer K, Kramer F, Spiller DG, Richardson RV, Chapman KE, Farrow SN, Norman MR, Williamson AJ, Whetton AD, Taylor SS, Tuckermann JP, White MR, Ray DW. Glucocorticoid receptor regulates accurate chromosome segregation and is associated with malignancy. Proc Natl Acad Sci U S A. 2015 Apr 28;112(17):5479-84. doi: 10.1073/pnas.1411356112. Epub 2015 Apr 6. PMID: 25847991; PMCID: PMC4418855.
71. Miltenyi Biotec. Satellite Cell Isolation Kit. Mouse. https://www.miltenyibiotec.com/upload/assets/IM0009000.PDF
72. Fisher GJ, Varani J, Voorhees JJ. Looking older: fibroblast collapse and therapeutic implications. Arch Dermatol. 2008 May;144(5):666-72. doi: 10.1001/archderm.144.5.666. PMID: 18490597; PMCID: PMC2887041.
73. Rajgara, R. (2023). *The Role of Glucocorticoid Signaling in Adult Muscle Stem Cell and Myogenic Differentiation.* (Doctoral thesis, University of Ottawa). http://dx.doi.org/10.20381/ruor-29269
74. Belanto JJ, Diaz-Perez SV, Magyar CE, Maxwell MM, Yilmaz Y, Topp K, Boso G, Jamieson CH, Cacalano NA, Jamieson CA. Dexamethasone induces dysferlin in myoblasts and enhances their myogenic differentiation. Neuromuscul Disord. 2010 Feb;20(2):111-21. doi: 10.1016/j.nmd.2009.12.003. Epub 2010 Jan 18. PMID: 20080405; PMCID: PMC2856642.
75. Yang YC, Lin CH, Lee EH. Serum- and glucocorticoid-inducible kinase 1 (SGK1) increases neurite formation through microtubule depolymerization by SGK1 and by SGK1

phosphorylation of tau. Mol Cell Biol. 2006 Nov;26(22):8357-70. doi: 10.1128/MCB.01017-06. Epub 2006 Sep 18. PMID: 16982696; PMCID: PMC1636775.
76. Kodani A, Sütterlin C. The Golgi protein GM130 regulates centrosome morphology and function. Mol Biol Cell. 2008 Feb;19(2):745-53. doi: 10.1091/mbc.e07-08-0847. Epub 2007 Nov 28. PMID: 18045989; PMCID: PMC2230605.
77. Bexiga, Mariana & Simpson, Jeremy. (2013). Human Diseases Associated with Form and Function of the Golgi Complex. International journal of molecular sciences. 14. 18670-81. 10.3390/ijms140918670.
78. Reul JM, de Kloet ER, van Sluijs FJ, Rijnberk A, Rothuizen J. Binding characteristics of mineralocorticoid and glucocorticoid receptors in dog brain and pituitary. Endocrinology. 1990 Aug;127(2):907-15. doi: 10.1210/endo-127-2-907. PMID: 2164924.
79. Rimmele U, Besedovsky L, Lange T, Born J. Blocking mineralocorticoid receptors impairs, blocking glucocorticoid receptors enhances memory retrieval in humans. Neuropsychopharmacology. 2013 Apr;38(5):884-94. doi: 10.1038/npp.2012.254. Epub 2012 Dec 6. PMID: 23303058; PMCID: PMC3671995.